BNEN Master Thesis - Non-Confidential Version

Neutronic coupling between the MYRRHA core and the In-Vessel Fuel Storages

Stefano Benedetti

Academic year 2010-2011

Promotor: Dr. Ir. Peter Baeten

Assessors: Pr. Ir. Pierre Van Iseghem / Pr. Sandra Dulla

Mentor: Dr. Alexey Stankovskiy

Thesis submitted in partial fulfilment
of the requirements for the degree of
Master of Science in Nuclear
Engineering

Copyright

All property right and copy right are reserved. Any communication or reproduction of this document and any communication or use of its contents without explicit authorisation is prohibited. Any infringement to this rule is illegal and entitles to claim damages from the infringer, without prejudice to any other right in case of granting a patent of registration in the field or intellectual property.

© BNEN, Belgian Nuclear Education Network [1]

[1] BNEN is a consortium of the Belgian universities *Katholieke Universiteit Leuven (K.U.Leuven), UniversitÃl catholique de Louvain (UCL), UniversitÃl de LiÃlge (ULg), Universiteit Gent (UGent), Vrije Universiteit Brussel (VUB),UniversitÃl Libre de Bruxelles (ULB)* in collaboration with the *Nuclear Research Centre SCK•CEN.*

Administration Manager BNEN: Thomas Berkvens c/o SCK•CEN, Boeretang 200, B-2400 MOL, Belgium.

Master of Science in Nuclear Engineering

Thesis Summary Page

Name of the student:

Stefano Benedetti

Title:

Neutronic coupling between the MYRRHA core and in-vessel fuel storage

Abstract:

A Multi-purpose Hybrid Research Reactor for High-tech Applications (MYRRHA) is being developed in SCK·CEN. The 100 MWth fast reactor core is designed to operate both in critical and subcritical (driven by 600 MeV protons from an accelerator) mode. The reactor will have a pool design where the lead-bismuth eutectic (LBE) serves as a coolant and spallation target.

Spent fuel still generates decay heat and must remain in the coolant for some time after the reactor is shut down. To avoid excessive delay between two operation cycles, it was chosen to store the spent fuel at the periphery of the reactor. There are two fuel storage zones previewed in the pool. They together are capable to store two fuelled cores or one complete core, and ~ 10 absorbing assemblies.

The influence of these storages on the core neutronic performance will be the subject of the study. Both normal and accidental conditions will be investigated. The induced fission power in the storage due to neutrons leaking from the core will be calculated as well. The neutronic analysis will be carried out with MCNPX general purpose Monte Carlo radiation transport and ALEPH Monte Carlo burnup codes.

Promotor: Dr. Ir. Peter Baeten Approval for submission by promotor:

Mentor: Dr. Alexey Stankovskiy

Assessors: Pr. Ir. Pierre Van Iseghem – Pr. Sandra Dulla

Academic Year 2010 - 2011

Belgian Nuclear Higher Education Network, c/o SCK•CEN, Boeretang 200, BE-2400 Mol, Belgium

Preface to the Non-Confidential Version

In writing the present thesis, I had the luck to work in a challenging and stimulant research environment, giving a small contribution to the development of the MYRRHA design.

For confidentiality reasons, not all the work I have accomplished could be published outside the SCK•CEN. As a matter of fact, the present version does not contain an Appendix, where I have described the geometry of MYRRHA and the calculation methodologies adopted. All the rest of the work is remained unchanged.

Stefano Benedetti
Rovereto, July 2011

Preface

The recent Fukushima accident has sparked off a renew fear in the public opinion towards the nuclear technology. Moreover, still many open issues remain to face, such as the extremely long life of nuclear wastes, in order to reach a widespread public acceptance of this technology.

For these reasons, research efforts of new nuclear reactors is strongly needed. The MYRRHA project, designed at the SCK•CEN since 1998, will represent a cutting edge technology that will contribute to plug this gap. Among its many innovative applications, MYRRHA will be able to test the feasibility of nuclear waste transmutation, namely to shorten the life-time of nuclear wastes.

The present thesis aims to bring a small contribution to the design of MYRRHA, by investigating the neutronic behaviour of the In-Vessel Fuel Storages and their interaction with the reactor core. Each chapters have been structured with clear introduction and conclusion, in order to be easily understandable. It is hoped that the found results will be of value to the readers.

Stefano Benedetti
Rovereto, July 2011

Acknowledegements

Many people have contributed to this thesis. I especially would like to thank my promoter, Peter Baeten, and my mentor, Alexey Stankovskiy for their great help and kindness during the realization of this work. Without their contribution this thesis would have never seen the light of the day.

My gratitude goes also to my assessors, Pierre Van Iseghem and Sandra Dulla, for their precious suggestions, and to Gert Van den Eynde, who greatly contributes to solve my doubts as well.

A special thanks to all the new friends I found during this amazing year abroad. This experience has changed me a lot, hopefully for the better, and this is mainly due to all of you.

My final thanks is to my family, for having always stood by me.

Stefano Benedetti
Rovereto, July 2011

Contents

Summary

MYRRHA will be an innovative nuclear reactor that is currently under designed at the SCK•CEN research centre in Mol. Among its many peculiarities, MYRRHA will be a pool reactor, lead bismuth eutectic cooled. At the reactor periphery, four In-Vessel Fuel Storages are forecast, in order to store both fresh and spent fuel assemblies, together with other sub-assemblies.

This thesis is dedicated to the study of the neutronic behaviour of the In-Vessel Fuel Storages. The model adopted considers the 68 fuel assemblies 100 MW_{th} critical core, loaded with MOX fuel with 33 wt.% Pu in heavy metal. The analysis has been mainly carried on by using the general purpose Monte Carlo radiation transport code MCNPX together with the point-wise JEFF-3.1.1 data library.

After a short introduction, intended to provide the basic general information on MYRRHA, in the second chapter the neutronic coupling between the INVFS's and the reactor core has been investigated. It has been proved that we do not experience neutronic coupling in any operating condition. The criticality of the INVFS on his own has been also calculated. It has been verified that the safe limit of effective neutron multiplication factor equal to 0.95 is not exceeded. A similar study has been accomplished in the past by the ITN group. The present work is in accordance with those calculations.

The third chapter deals with the neutronic flux and thermal power distribution in the In-Vessel Fuel Storages. The fuel assemblies have been analyzed considering first the fissile part only, and later the whole hexagonal cylinder. Due to the symmetry of the problem, only one out of the four INVFS's has been analyzed. The neutron flux in them is considerably lower, about two order of magnitude, than the one present in the core. The distribution is strongly asymmetric, showing that the neutron flux is basically induced by the neutrons that leak from the core. The power generation is consequently lower that the one in the core. Considering a total loading with fresh fuel assemblies, the thermal power of one INVFS during the reactor operation at maximum power is equal to approximately 1 MW. The analysis of the axial distribution of the flux/power has shown that we experience a good homogeneity of that values along the vertical axis. A short analysis of the core has been carried on as well, in order to validate these results. The found values agree with the reference ones.

The fourth chapter tackles the burn-up issue. The general purpose Monte Carlo burn-up code ALEPH has been used in this analysis. Due to the high asymmetry of the neutron flux distribution in the INVFS's, three different irradiation condition has been considered. Consequently, three average burn-up zones are present in the model. In the analysis, 90 days irradiation and 30 days of decay have been taken into account, following the forecast schedule of operation of MYRRHA. Fresh fuel stored in the INVFS's does not

show a significant evolution of the thermal power and of the burn-up during the 90 days of operation, proving a small depletion of the fissile material. The composition evolution of the fuel, accordingly, is rather constant. The major depletion is undergone by the Pu-241, which decreases of the 1.52 % on weight. The activity is almost six times higher during operation, but due to the limited build-up of fission products and minor actinides, soon relaxes on the initial one in the 30 days of decay. The major contribution to the overall activity during operation comes form the fission products. Irradiated fuel already shows a significant depletion, due to its location in the reactor core under much harder neutronic conditions. As a matter of fact, no significant evolution in the thermal power, burn-up and composition is observed. The activity, due to the high presence of fission products, keeps on decreasing also during operation, due to the relatively lower neutron flux with respect to the core.

The last chapter aims to provide an introductory analysis of several accidental conditions that could occur in both the INVFS's and in the core. In this case, only a fresh fuel assemblies loading has been considered, since it represents the most severe situation. Various scenarios have been tackled, such as the loss of the cladding, the melting of the fuel and its re-compaction as an unique block in different location of the core/INVFS, the partial loss of LBE around the FAs, and the total loss of LBE in the reactor pool. The feasibility of these scenarios has not been investigated, since we were interested in the neutronic behaviour of the system. Different levels of damage have been considered as well, ranging from only one fuel assemblies spoiled, up to all the core/INVFS. Both the loss of the cladding and the appearance of void coefficient in the LBE does not lead to significant change in the reactivity of the core. On the contrary, much more severe situation is encountered when we consider the melting and relocation of the fuel in a compact block inside the hexagonal lattice. In these cases, the increased in the reactivity is significant, both when this scenario happens in the core and in the INVFS's. Regarding the last case analyzed, namely the total loss of the LBE, it has been showed that we experience in this case a strong reduction of the reactivity of the reactor, due to the much higher neutron leakages.

Finally, several Appendixes complete this work. It has been chosen on purpose to make wide use of this instrument, in order to lighten the exposition of the results and their discussion in the body of the master thesis. The first Appendix, that has been canceled for confidentiality reasons in the non-confidential version, explains the calculation methodologies adopted and the main geometry dimensions of MYRRHA. Appendix B is a short overview on the reliability of Monte Carlo calculations, while Appendix C explains briefly the ALEPH model. Lastly, Appendix D contains a small technical report written in parallel with the thesis, which has been decided to enclose to it as a small "extra-work".

List of abbreviations and symbols

ADS	Accelerator Driven System
BoL	Beginning of Life
BR1	Belgian Reactor 1
BR2	Belgian Reactor 2
BR3	Belgian Reactor 3
CR	Control Rod
EoL	End of Life
ERANOS	European Reactor ANalysis Optimized calculation System
FA	Fuel assembly
FASTEF	FAst Spectrum Transmutation Experimental Facility
FOM	Figure of Merit
IPS	In Pile Sections assemblies
ITN	Instituto Tecnolologico e Nuclear
MCNPX	Monte Carlo N-Particle eXtended transport code
MYRRHA	Multi-purpose hybrid research reactor for high-tech applications
INVFS	In vessel fuel storages
LBE	Lead Bismuth Eutectic
MC	Monte Carlo
MOX	Mixed OXide fuel
SA	Sub-Assemblies
SR	Safety Rod
SCRAM	Safety Control Rod Axe Man
k_{eff}	Effective neutron multiplication factor
ρ	Reactivity

List of Tables

List of Figures

Chapter 1

Introduction

The Belgian nuclear research centre or studiecentrum voor kernenergie - centre d'étude de l'énergie nucléaire (SCK•CEN) was founded in 1952 in order to "carry out all research regarding applications of nuclear power and to promote and encourage such research by any means possible" [1].

From 1952, three research reactor have been built inside the SCK-CEN research centre, namely:

- the Belgian Reactor 1 (BR1), a graphite moderated, air cooled reactor, which became critical for the first time in 1956;
- the Belgian Reactor 2 (BR2), a beryllium matrix, water moderated high flux reactor, loaded with highly enriched uranium; it became critical for the first time in 1961;
- the Belgian Reactor 3 (BR3), the first PWR built outside the USA, which became critical in 1962; the BR3 was decommissioned and dismantled in 1987.

In 1998, a feasibility study for the construction of a new reactor have been launched, with the purpose of replacing the BR2 reactor and having a even more powerful research reactor, with higher neutron fluxes and energies. The project has been named MYRRHA, which stands for Multi-purpose hYbrid Research Reactor for High-tech Applications.

1.1 MYRRHA: an overview

MYRRHA will be a flexible fast spectrum irradiation facility able to operate in sub-critical and critical mode [2]. In the sub-critical configuration, a high-energy proton beam will impinges on the lead-bismuth eutectic that cool down the core, causing spallation and driving the reactor to a critical state.

The three main goals of this new reactor are:

- to demonstrate the ADS feasibility at a reasonable power level;
- to study the transmutation of high-level nuclear wastes, with special interest for the long-lived, namely the minor actinides;

- to operate as a flexible fast spectrum facility, to allow, under a very harsh neutron spectrum, new fuel and material developments, together with radioisotope production for medical applications and industrial applications, such as Si-doping.

The public opinion often forgets the extreme importance of such facilities in our everyday lives. For instance, modern medicine makes wide use of radioisotopes, like Tc-99m, in the diagnostic activity and in the cure of various illness, among which tumors. From this perspective, MYRRHA represents an essential instrument to keep on ensuring the necessary production of these elements.

However, the most ambitious goal of MYRRHA will be the study of the transmutation of nuclear wastes. Current nuclear reactors produce two type of wastes, the minor actinides and the fission products. By transmutation, the minor actinides and the long-lived fission products are turned into isotopes which have an average life-time of approximately 300 years, on the contrary to the present average of billion of years. This should lead to a broader acceptance of the nuclear technology in the public opinion.

The MYRRHA project underwent several evolution since 1998. The latest version refers to the acronym FASTEF. The principal parameters are listed in Table 1.1.

Core external diameter	1450 mm
Core height	2000 mm
Fuelled length	600 mm
Vessel diameter	7500 mm
Vessel total height	13000 mm
Vessel cover thickness	2000 mm
Gas plenum	500 mm
Nominal power	100 MW
Core inlet temperature	270 °C
Core outlet temperature	410 °C
Coolant velocity in the core	2 m/s
Secondary coolant	Steam

Table 1.1: MYRRHA FASTEF parameters [3]

1.1.1 Main components

This section is not intended to give a full description of the MYRRHA components, but rather to provide a first insight on this new facility.

Figure 1.1 shows an overview of the reactor, with its main components, listed on the right-hand side label.

The central critical (or sub-critical) core will be surrounded, mainly, by:

- 4 heat exchangers;
- 2 primary pumps;
- 4 in-vessel fuel storages;

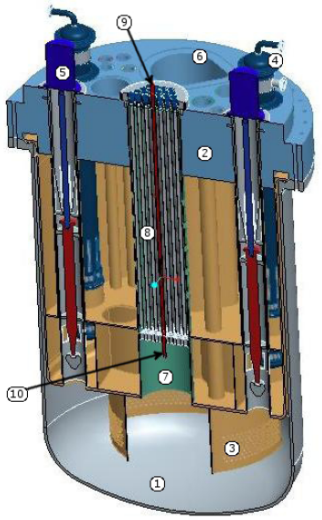

Figure 1.1: Overview of the MYRRHA-FASTEF reactor [4]

- 2 in-vessel fuel handling machines.

The central critical core houses 151 assemblies position, filled with fuel assemblies, control rods, scram rods, the spallation window, in-pile sections, reflector assemblies, instrumentation and surveillance capsules. The various assemblies are loaded in the core from underneath, by means of the two in-vessel fuel handling machines, which cover one half of the core each. An important peculiarity of this new reactor is that, thanks to the buoyancy, fuel and reflector assemblies do not need to be locked on the core support plate.

From a thermo-hydraulic point of view, the two pumps force the LBE from the low pressure hot plenum above the diaphragm through the four heat exchangers and eventually back to the cold high pressure underlying plenum.

When the reactor will be operated in the sub-critical mode, a proper penetration from the top of the reactor will lead the proton beam to the centre of the core, down to the spallation window.

Several critical configurations of the core have been designed, at different level of power. In the present work, a 68 FAs 100 MW_{th} critical core has been considered. Further description of the the MYRRHA design can be found in the Appendix A of the confidential version.

1.2 The neutronic coupling issue

A brief description of the main components and dimensions of MYRRHA has been discussed in the previous section. Fissile material inside the reactor vessel can be placed in the core, but also in the four In-Vessel Fuel Storages. The INVFS have been designed in order to [4]:

- remain sub-critical in any operating condition, with $k_{eff} < 0.95$;
- not modify the k_{eff} of the core, namely to not have neutronic coupling with it.

The main goal of the present thesis was the verification that these requirements were satisfied. Besides that, in the following chapters the characterization of the neutron flux and of the thermal power generated in the INVFS's have been accomplished, together with the investigation of the depletion's level of the fissile materials stored in the INVFS's during the 90 days of irradiation [see Figure B.1]. Finally, several accidental scenarios have been simulated, both affecting the core and the In-Vessel Fuel Storages.

It has been chosen to make wide use of the appendixes, with the aim of lighten the presentation of the results and their conclusions. Consequently, most of the calculation methodologies are explained separately.

Appendix C represents a small "extra-work" carried on in parallel with the thesis that has been decided to enclose to it.

Chapter 2

Criticality calculations

2.1 Introduction

In order to maintain a self-sustained chain reaction in the reactor, the number of neutrons that is produced must be equal to the number of neutrons that is absorbed or leak. This intuitive concept is well defined by the effective multiplication factor, which is the ratio of the number of fissions in any one generation to the number of fissions in the immediately preceding generation [5]. If the effective multiplication factor (symbol k_{eff}) is equal to one, the system is said to be critical. That means that the reactor is stable at a certain power, namely the chain reaction just sustains itself.

Another important parameter link with the neutron multiplication factor is the reactivity of a reactor, symbol ρ. The reactivity is expressed by the following equation:

$$\rho = \frac{k_{eff} - 1}{k_{eff}}. \tag{2.1}$$

The critical condition is reached when the reactivity is equal to zero.

In this chapter we will tackle the criticality calculation of the core of MYRRHA, in order to verify whether the presence of the in-vessel fuel storages has an influence on the neutronic of the reactor.

2.2 The criticality calculation with MCNPX [6]

Several methods have been developed in order to calculate the criticality of a given reactor. Some of them are completely analytical, like the Fermi's six factor formula, some others make use of approximate models, like the diffusion equation, in order to find the value of the k_{eff}. Even by using the diffusion theory, which is the approximation of the correct but much more complicated transport theory, we are able to solve the problem in an analytical way only for very simple geometry.

Thus, the modern project of a reactor involves the utilization of computational codes, either deterministic (i.e. ERANOS) or probabilistic, like MCNPX.

MCNPX is a general purpose Monte Carlo radiation transport code designed to track many particles types over broad ranges of energies [6]. Thanks to its high capability, MCNPX is used in a very large number of scientific fields, such as nuclear medicine, nuclear safeguards, accelerator applications, homeland security and nuclear criticality [7]. It is the main computational tool adopted in the developing of the present thesis.

MCNPX computes the k_{eff} by estimating the mean number of fission neutrons produced in one generation per fission neutron started. A generation is considered terminated when all the fission neutrons born have either escaped, undergone parasitic captures or absorptions that lead to fissions. Thus, from the previous definition, we have:

$$k_{eff} = \frac{\text{fission neutrons in generation i+1}}{\text{fission neutrons in generation i}} = \\ = \frac{\rho_a \int_V \int_0^\infty \int_\Omega \nu\sigma_f \Phi dV dt dE d\Omega}{\int_V \int_0^\infty \int_E \int_\Omega \nabla \bullet J dV dt dE d\Omega + \rho_a \int_V \int_0^\infty \int_E \int_\Omega (\sigma_c + \sigma_f + \sigma_m) \Phi dV dt dE d\Omega} \text{ [6].} \tag{2.2}$$

The previous equation, apparently complicated, is indeed a simple balance equation that comes from the Boltzmann transport equation in absence of external source: the denominator considers the loss rate, sum of leakage (first term), capture, fission and multiplicity (n,xn) (second term), while the numerator represents the source term.

2.3 The effective neutron multiplication factor of the MYRRHA core

In this master thesis work, two main MCNPX input files have been used for the description of the model used. The first one is the reference input file for the critical configuration of the core, developed by NSP group of the ANS at the SCK•CEN. It contains the description of the critical core and the pool of the reactor. A picture of the critical core of MYRRHA [see Section 1.1.1] taken from MCNPX is shown in Figure 2.1.

The first job to perform was a simply running of the input file, in order to compute the neutron multiplication factor of the system with this configuration. Table 2.1 shows the result of this calculation.

k_{eff}	Standard deviation (pcm)
1.05269	0.00006

Table 2.1: Effective neutron multiplication factor of the critical MYRRHA core

It is important to point out that this result has been obtained with the SCRAM rods and the control rods fully withdrawn, and at BoL. Thus, the small excess of reactivity would be easily controlled. Further information about the methodology adopted in the calculations can be found in the Appendix A of the confidential version.

All the found results refer to a critical core at BoL, in a cold geometry model, namely we do not consider the dilatation of the materials, but in hot operating conditions. According to [8], the use of a model with cold geometry and density leads to an over-estimation of the k_{eff} of the core of ≈ 500 pcm. The present results are a bit more refined, because we

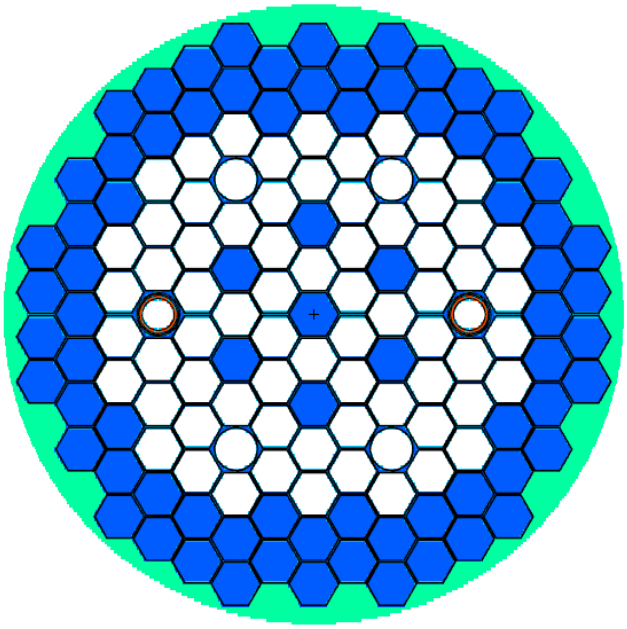

Figure 2.1: Critical core of MYRRHA

take into account hot operating condition. Thus, we expect that in a real "hot" geometry our k_{eff} is between 0 and 500 pcm lower.

MYRRHA will be a pool reactor, so the project forecast the presence of several element inside it. Since the major contribution to the change of the neutronic of the system will arise from the presence of the INVFS's, the reference input file was modified considering also the presence of the four in-vessel fuel storages.

The geometry characteristics of them were taken by another input file developed inside the SCK-CEN. Here follows a picture of the MYRRHA core together with the four in-vessel fuel storages [Figure 2.2].

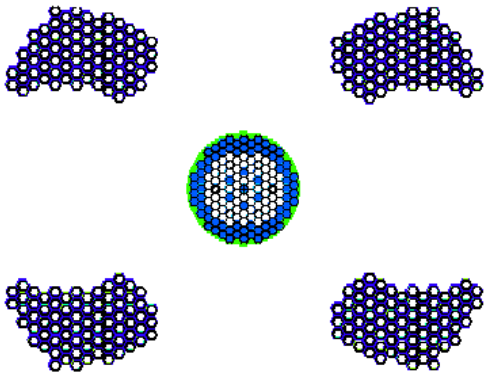

Figure 2.2: Critical core of MYRRHA with four INVFS's

The in-vessel fuel storages are forecast to accommodate both fresh and spent fuel, and also other kind of assemblies, for instance material testing assemblies. Goal of this chapter is to verify the behaviour of the system in the worst case scenario, namely when all the INVFS's are loaded with fresh FAs.

Indeed, a loading scenario with both the core and the four INVFS's fully loaded with fresh fuel assembly will never be reached. In fact, this would not allow to unload the core at the end of the operating period, unless a previous unloading of the INVFS's have been carried on. Nevertheless, we will see that not only the In-Vessel Fuel Storages do not affect the neutronics of the core, but they do not affect each other even. That's the reason why the analysis have been fulfilled considering all the four INVFS's fully loaded with fresh or spent fuel.

The provided input file containing the description of the INVFS's is written considering cold geometry and operating conditions, apart from the fuel, which is considered to be at 1500 K. Several assumptions on the temperature of the various materials in the INVFS's have been done, which are summarized in the Appendix A, confidential version.

Here I would like to point out that the following results are based on these assumptions, which would require also some thermo-hydraulic calculations to well defined the various temperatures. A simple sensitivity analysis of the results on the fuel temperature will be presented in Section 2.6.

With this configuration, the following results have been obtained [Table 2.2].

k_{eff}	Standard deviation (pcm)
1.05266	11

Table 2.2: Effective neutron multiplication factor: critical MYRRHA core with four INVFS's loaded with fresh fuel assemblies

The difference in the neutron multiplication factor between the two system is of 3 pcm lower. Considering that the standard deviations of our result are 6 and 11 pcm, we can state that our system does not show a statistical significant neutronic coupling.

From the previous calculation, we know that the storage of fresh fuel assemblies in the INVFS's does not lead to sensible changes in the reactor reactivity. It is interesting however to verify if the same condition is achieved with spent fuel in the INVFS's instead of the fresh ones, or if we have a not negligible negative effect on the reactivity.

The considered spent fuel has spent five cycles in the reactor. From Table B.1, we can easily calculate that the fuel has been irradiated for 450 days in total, with 210 days of decay. Table 2.3 shows the found results.

k_{eff}	Standard deviation (pcm)
1.05262	12

Table 2.3: Effective neutron multiplication factor: critical MYRRHA core with four INVFS's loaded with spent fuel assemblies

We have thus demonstrated that also in this case the effects are negligible, since the difference with the reference core is equal to 7 pcm, well inside the confidence interval.

2.4 The effective neutron multiplication factor under SCRAM condition

The adopted model of the core, as widely explained in Appendix A, confidential version, foresees 68 FAs, 4 control rods and 2 SCRAM, together with 7 central IPS's. If the SCRAM signal is given, all the six control rods are completely inserted in the core, leading to a sub-critical state of the reactor.

We have previously seen that the presence of the INVFS's does not affect greatly the neutronic of the reactor. Nevertheless, let's now verify whether under SCRAM condition the system remains sub-critical in both the two cases. The values of the k_{eff} found for both the core alone and the core with the four INVFS's are shown in Table 2.4.

	k_{eff}	Standard deviation (pcm)
MYRRHA reference core	0.90003	5
MYRRHA core + 4 INVFS's	0.92300	12

Table 2.4: Effective neutron multiplication factor of the reactor under SCRAM condition

Not surprisingly, when we consider the presence of the INVFS's the value of the k_{eff} is bigger. In this latest more realistic situation however, the safety system is still capable to introduce in the reactor an anti-reactivity equal to ≈ 8340 pcm [see Eq. 2.1].

2.5 The effective neutron multiplication factor of the INVFS

Another goal of this chapter is the evaluation of the neutron multiplication factor of the INVFS's only. This is necessary in order to verify that we maintain ourselves sufficiently far away from the criticality when we deal with fresh fuel loaded only in the INVFS's.

To perform this calculation, rather than get rid of the whole core, which is not a realistic possibility, two different situations have been considered:

- replacement of the SAs in the core with LBE;
- replacement of the whole core with dummy FAs, filled with LBE.

The two configurations are pretty similar from a neutronic point of view. However, the two calculations will allow us to see if in the second case the presence of an higher amount of structural materials will affect significantly the results.

The melting temperature of the LBE is, at atmospheric pressure, around 398 K [9]. Nevertheless, it has been chosen to run the present calculation with all the materials at room temperature, namely 300 K. This is, as we have previously discussed, the most conservative situation, so the verification of the sub-criticality of the system with these assumptions would guarantee the sub-criticality in any conditions.

The results are summarized in Table 2.5.

As we can see, the two simulations do not show a significant difference. The found results are lower than the safe limit of $k_{eff} = 0.95$ that is considered the upper bound to remain in a safety configuration [10].

	k_{eff}	Standard deviation (pcm)
Only LBE in the core	0.92952	11
Only dummy assemblies in the core	0.92956	11

Table 2.5: Effective neutron multiplication factor of the INVFSs

2.6 Sensitivity analysis

A comprehensive sensitivity analysis of the obtained results has not been carried on. However, while the temperature in the core has been considered to be correct, the effect of the temperature change of the fuel present in the INVFS's has been analyzed. All the other parameters, such as temperature of the LBE, have not been changed. As a matter of fact, all the materials have been considered in thermal equilibrium with the LBE average pool temperature of 550 K, and the fuel has been set at 600, 900 (our reference temperature), 1200 and 1500 K (the fuel temperature in the core).

Table 2.6 summarizes the obtained results.

Temperature (K)	k_{eff}	Standard deviation (pcm)
600	1.05272	11
900	1.05266	11
1200	1.05234	11
1500	1.05263	12

Table 2.6: Sensitivity analysis results

A clear trend is thus not visible. However, in the present calculation we are only considering the change in the fuel temperature of the INVFS's, that, we have seen it before, have a very little influence on the overall reactor criticality.

As a rule of thumb, from previous calculations and from the reactor theory (Doppler effect), we can say that the lower the fuel temperature considered, the higher is the reactivity of the system.

2.7 Validation of the results

As previously stated, the found results refer to a critical core at BoL, in a cold geometry model. The temperatures adopted are listed in the Appendix A of the confidential version.

Referring to the criticality calculation of the core, a work at cold density has been carried on by using ERANOS, a deterministic neutronic code. The value of the k_{eff} found in such a way was equal to 1.04692 [11].

Another work, performed by the ITN group, dealt with the criticality of the INVFS's and has tackled the neutronic coupling issue, using MCNPX as well. This group has considered the reactor working at room temperature, in a cold geometry model, except for the fuel, that for both the core and the INVFS's has been set up at 1500 K.

It has been found a value for the k_{eff} equal to 0.92507 $\pm$ 0.00058 at 300 K [12]. The difference with the present results is thus of about 400 pcm. However, the present results

take into account realistic operating temperatures, and so should describe more accurately the real system.

A criticality coupling calculation was also carried on, but considering only 76 FAs located in one INVFS. The value of the k_{eff} found is equal to 1.05893 ± 0.00061. Considering only the core, the ITN group has found a value of the k_{eff} equal to 1.05931 ± 0.00067.

2.8 Conclusion

In this chapter the results of the criticality calculations performed on MYRRHA have been presented.

The major conclusion is that we do not experience any kind of neutronic coupling issue between the core and the INVFS's. Also considering a SCRAM condition, the system is perfectly capable to drive the reactor into a sub-critical state. However, the presence of fresh loaded INVFS's affect in this case significantly the overall behaviour of the reactor. Finally, the criticality of the INVFS's alone has been investigated. The found results are far from the $k_{eff} = 0.95$ safe limit, thus the safety designed of the INVFS's has been proved.

Table 2.7 summarizes the found results.

	k_{eff}	Stand. dev. (pcm)
Operating condition		
Critical reference core	1.05269	6
Core + INVFS's (Fresh fuel loaded)	1.05266	11
Core + INVFS's (Spent fuel loaded)	1.05262	12
SCRAM condition		
Critical reference core	0.90003	5
Core + INVFS's	0.92300	12
INVFS' criticality		
Four fresh fuel loaded INVFS's	0.92952	11

Table 2.7: Summary of the results of Chapter 2

The obtained results have been compared with similar works performed in the past. The results are in accordance with those calculations.

A simple sensitivity analysis has been carried on, showing that the uncertainty on the fuel temperature in the INVFS's stored FAs does not lead to significant errors in the calculation.

Chapter 3

Heat generation in the INVFS

3.1 Introduction

In the previous chapter we have dealt with the criticality analysis of the core of MYRRHA. The main conclusion of that work was that we do not have neutronic coupling between the core and the in-vessel fuel storages. Nevertheless, it is important to verify what is the level of the neutron flux and of the heat generation in the INVFS's.

In this chapter this topics will be tackled. The INVFS's will be loaded with both fresh or spent fuel, or a combination of them. Since the most severe situation is achieved when we have a complete fresh fuel loading, only the results of such a scenario will be presented. An approximative analysis on the heat generation of spent fuel in the INVFS's will be presented in the next chapter.

In this chapter we have analyzed the 100 MW critical core with 68 FAs, at BoC. As we have previously seen, the system is super-critical, with a $k_{eff} \approx 1.05$. We did not take into account the partial insertion of the CRs to compensate for the initial extra-reactivity. Thus the peaking factors referred to the core could be a bit under-estimated.

While is performing a criticality calculation, MCNPX normalizes any tallies that the user requests to the starting weight, which in our case is one fission neutron [13]. It is then necessary to scale the obtained results for an appropriate fission neutron generation rate [see Eq. 3.1].

$$P(MW) = C(\frac{MJ}{MeV}) \times Q(\frac{MeV}{fission}) \times F(\frac{fission}{neutron}) \times S(\frac{neutron}{second}). \tag{3.1}$$

So, the fission neutron generation rate can be easily computed once is known:

- the steady-state power at which the reactor is forecast to work (100 MW in the case of MYRRHA),
- the average energy release per fission (the average value calculated from Q-values for each nuclide weighted with the number of fissions occurred on each nuclide is 207.3 MeV/fission, taking into account fissions from both prompt and delayed neutrons, and the gamma heating),

- the average percentage of fission induced per neutron absorbed (data provided by the MCNPX output),
- the multiplication coefficient equal to $1.602 \times 10^{-}19\, MJ/MeV$.

The found value, which has been used in all the following calculations, is equal to 8.42621 E+18 neutrons/second.

MCNPX is able to provide the user with information about the flux and the energy deposition over a certain volume of known mass. Thus the units of measure are particles/cm^2 for the flux and MeV/g for the energy deposition. By multiplication with the source strength, expressed in neutron/second, we can obtain the correct values in particles/cm^{2}s and Watt/Kg.

In the following analysis we have made a symmetry assumption for our problem. This choice is completely reliable, since the geometry of the reactor is indeed symmetric. Thus only the results of the INVFS indicated in Figure 3.1 will be presented.

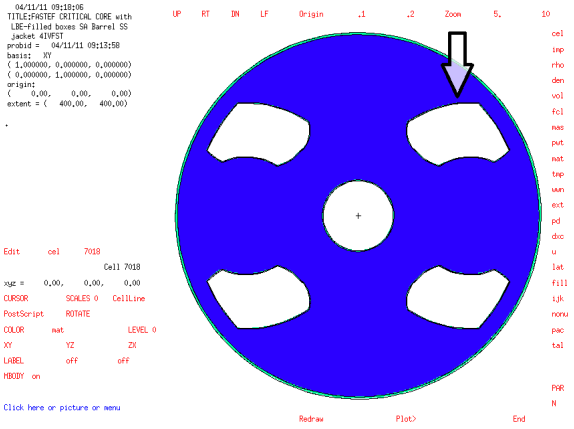

Figure 3.1: INVFS chosen for the calculations

3.2 Flux map of the INVFS

The knowledge of the neutron flux in the various region of a reactor represents the first challenge when people aims to build a nuclear facility. Once the neutron flux distribution is known, it is possible to compute the thermal power generation, for the termo-hydraulic calculations, and the flux induced damage to the structures of the reactor.

In the following chapter two different flux maps will be presented: the first relative only to the fissile part of the FAs, while in the second one the whole FA has been taken onto account.

3.2.1 Flux map of the fissile part

Figure 3.2 shows the flux map of the INVFS. It has been considered only the flux in the fissile material of the assembly, namely in the fuel pins.

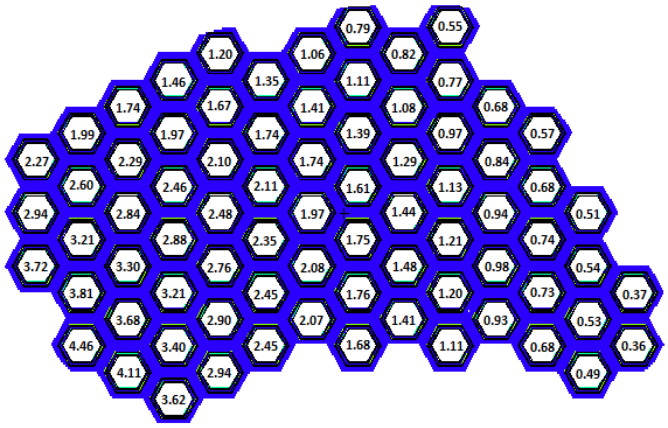

Figure 3.2: Flux map of the INVFS - Entire assembly, fissile part only. Values expressed in $10^{13} neutrons/(cm^2 s)$. Standard deviation between 1.5 and 0.5 %

In order to better characterize the flux distribution, the FA's have been vertically subdivided in three equal part. Figure 3.3 shows the values that refer to the central part of the assembly only, namely to a small volume with height 20 cm, ± 10 cm from the mid-plane.

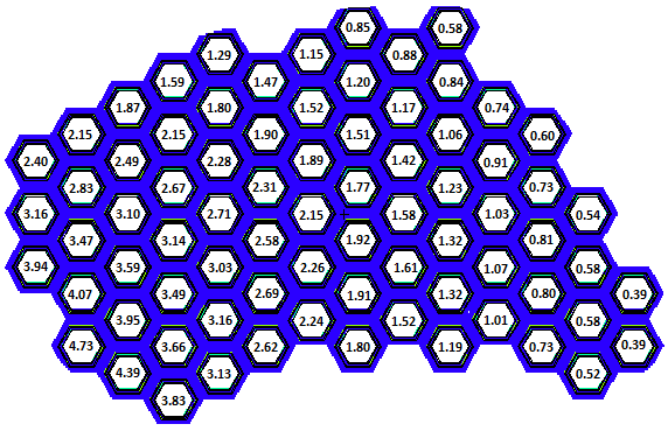

Figure 3.3: Flux map of the INVFS - Central part, fissile part only. Values expressed in $10^{13} neutrons/(cm^2 s)$. Standard deviation between 1.7 and 0.5 %

The uncertainties on the results are relatively high, especially for the less irradiated FAs, where the lower number of particles does not allow to reach precise statistical results. On the contrary, the results for the core are of course much more accurate.

Considering that the previous calculations have been runned with the stronger source [see Appendix A, confidential version], and that this has required almost seven days on the SCK-CEN cluster, a better definition of the results has been judged to be too time expensive. Moreover, considering the values found, more defined results are also in essence not necessary.

The main parameters that characterize the INVFS's flux distribution are summarized in Table 3.1.

[1]Ratio between the hottest FA and the average value
[2]Ratio between the value in the central part and the total flux

Maximum Flux	4.46E13 n/cm^2s
Minimum Flux	0.36E13 n/cm^2s
Average Flux	1.79E13 n/cm^2s
Max radial peak factor[1]	2.49
Highest axial peak factor	1.10
Axial peak factor in the most irradiated FA[2]	1.06

Table 3.1: Summary of the main neutronic parameters in the INVFS's

As it can be noticed, the flux is strongly related to the neutron irradiation exiting from the core. The strong flux difference between the FAs close to the core and the ones far form it will lead to different burn-up level. Nevertheless, we have to consider that, as we will see later, the flux in the INVFS's is two order of magnitude lower than the one in the core. In Chapter 4 the irradiation effect on the fuel of the INVFS's will be analyzed.

Regarding the difference between centre and top and bottom part of the fuel pins, we can notice that the flux is quite homogeneously distributed along the height.

The found results should be taken into account in the definition of the loading-unloading strategy of the reactor. That is, the spent fuel should be stored in the positions closer to the reactor, in order to act as a shielding with the respect to the fresh fuel, to be stored as far as possible form the reactor.

3.3 Flux map of the whole FA

To complete the discussion, let now see what is the flux map in the INVFS's considering the whole fuel assembly, instead of the fuel pins only. The volume over which the flux has been averaged is now the volume of a fuel assembly, namely an hexagonal cylinder with 4.8775 cm pitch and height equal to 140 cm. The flux map referred to the central part (± 10 cm from the midplane) and to the whole assembly are shown in Figure 3.4 and 3.5.

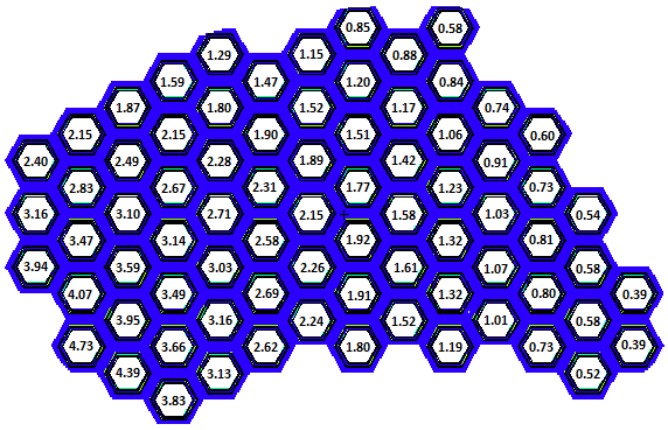

Figure 3.4: Flux map of the INVFS - Central part of the assembly. Values expressed in $10^{13} neutrons/(cm^2 s)$. Standard deviation between 0.9 and 0.5 %

These figures allow us to make some important considerations:

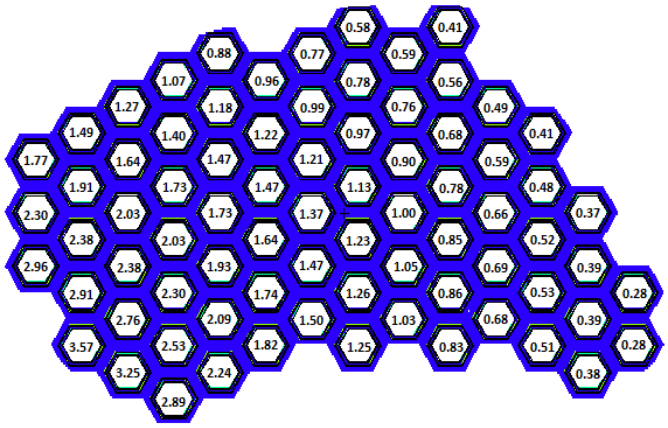

Figure 3.5: Flux map of the INVFS - Entire assembly. Values expressed in $10^{13} neutrons/(cm^2 s)$. Standard deviation between 1.6 and 0.5 %

- considering the central active part, the neutron flux basically does not change considering the fuel pins or the whole fuel assembly, on the contrary of what happens in the core; this means that, as we have seen in the previous chapter, the neutronic production in the INVFS's is negligible and the neutron flux is mainly driven by the neutrons that leak from the core;

- considering the whole fuel assembly (which consist of also non-active part, see Appendix A, confidential version), the flux remains relatively high, of the order of $10^{13} neutr/cm^2 s$, thus the activation of the materials and the structural related problem cannot be neglected.

Regarding the total flux distribution, the main parameters are summarized in Table 3.2

Maximum Flux	3.57E13 $n/cm^2 s$
Minimum Flux	0.28E13 $n/cm^2 s$
Average Flux	1.31E13 $n/cm^2 s$
Max radial peak factor	2.73
Highest axial peak factor	1.58
Axial peak factor in the most irradiated FA	1.32

Table 3.2: Summary of the main neutronic parameters in the INVFS's

3.4 Thermal power map of the INVFS

Together with the values of the flux, MCNPX is capable to provide the values of the power distribution as well.

Figure 3.6 shows the power distribution in the INVFS. We have considered the power generated by the fission in the fuel, which is the most important contributor.

From a thermo-hydraulic and structural point of view, it is also important to verify whether we have a significant axial power distribution along the pins height. Figure 3.7 shows the

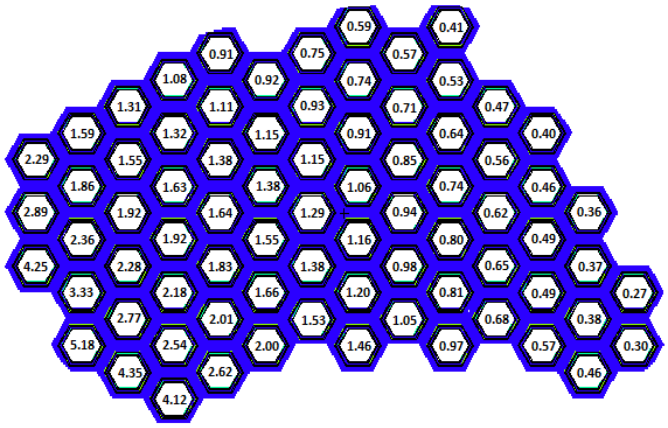

Figure 3.6: Power distribution in the INVFS - Entire assembly, fissile part only. Values expressed in $10^4 W$. Standard deviation between 1.2 and 0.5 %

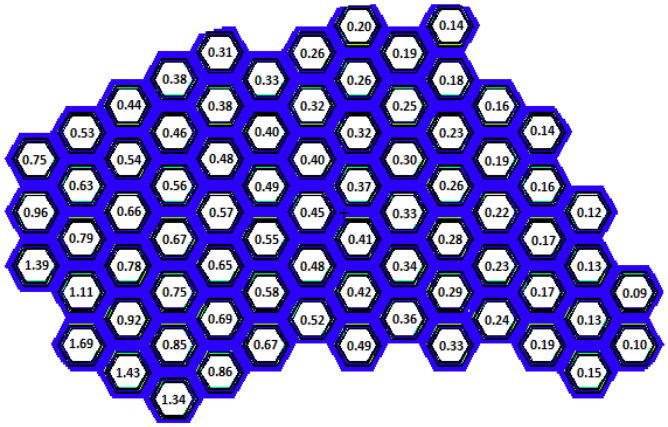

Figure 3.7: Power distribution in the INVFS - Central part, fissile part only. Values expressed in $10^4 W$. Standard deviation between 1.8 and 0.5 %

values that refer to the central part of the assembly only, namely to a small volume with height 20 cm, ± 10 cm from the midplane.

Table 3.3 summarize the results found.

Maximum power	51.76 KW
Average heat flux of the hottest FA[3]	20.32 W/cm^2
Minimum power	2.70 KW
Average power	13.75 KW
Max radial peak factor	3.76
Highest axial peak factor	1.07
Axial peak factor in the hottest FA	0.98
Total power	1045.38 KW

Table 3.3: Summary of the power parameters in the INVFS's

As we will see later, the hottest FA in the INVFS's has a power generation which is

[3]Through the total surface of the cladding

approximately 50 times lower than the one of the colder FA in the core. However, the four INVFS's, under the assumption that they are completely loaded with fresh fuel, generate approximately 4 MW_{th}.

The radial power distribution in the fissile zone is shown in Figure 3.8.

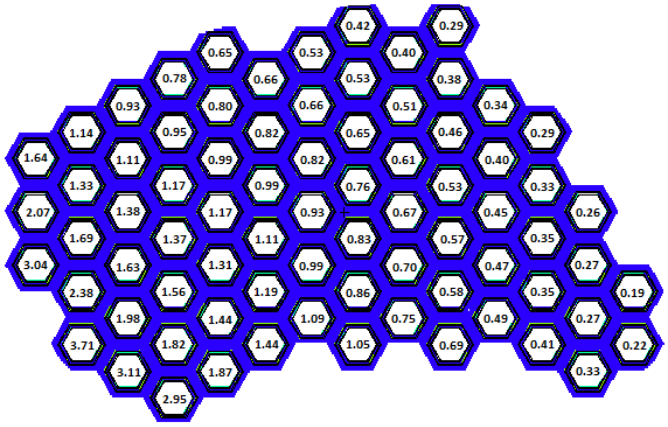

Figure 3.8: Power distribution in the INVFS fissile zone. Relative error ± 0.02

Figure 3.8 better shows the strong asymmetric distribution of the power in the FAs of the INVFS's. However, such high peaking factor should not represent a cause of concern, since the average values of flux and heat generation are relatively small.

In order to complete this thermal analysis, the thermal power map of the whole fuel assembly is shown in Figure 3.9. The same average condition considered in Section 3.3 has been taken into account. As it can be noticed, the differences with the previous power map are really minimal, proving again that the main contributor are the fission induced in the fuel by the nuetron leaking from the core. Table 3.4 summarizes these latest results.

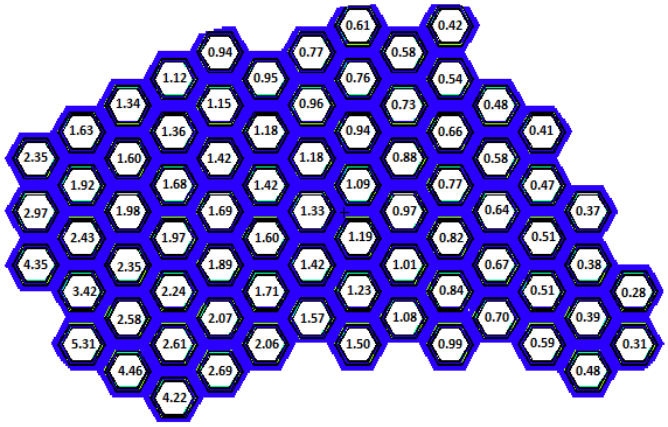

Figure 3.9: Power distribution in the INVFS - Entire assembly. Values expressed in 10^4 W. Standard deviation between 1.2 and 0.5 %

Maximum power	53.07 KW
Minimum power	2.79 KW
Average power	14.15 KW
Max radial peak factor	3.75
Total power	1075.47 KW

Table 3.4: Summary of the power parameters in the INVFS's

3.5 Flux map and power distribution of the core

The present thesis is supposed to be related to the characterization of the INVFS's only, since an exhaustive description of the core would require a deeper discussion. Nevertheless, in this section a flux map and a power distribution of the core will be presented, in order to validate the previous results and to provide a more complete overview of the subject.

Figure 3.10 shows the flux map of the core. It has been considered only the flux in the fissile material of the assembly, namely in the fuel pins.

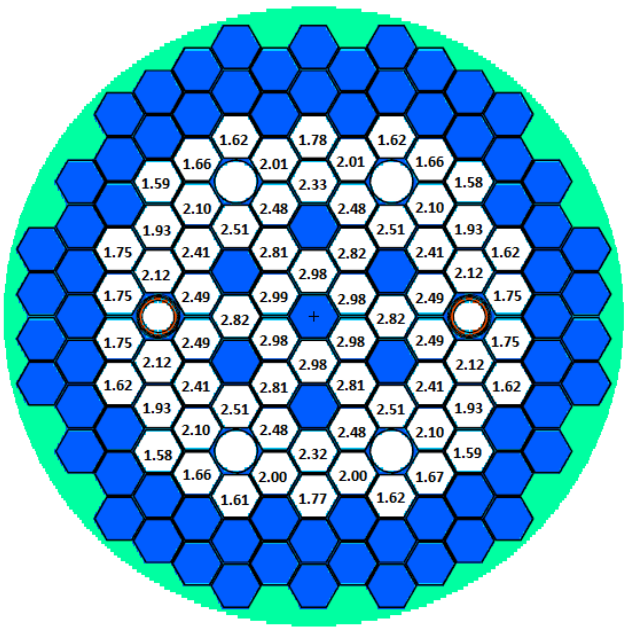

Figure 3.10: Flux map of the core - Entire assembly, fissile part only. Values expressed in $10^{15} neutrons/(cm^2 s)$. Max standard deviation 0.05 %

Figure 3.11 shows the power distribution in the INVFS. Again we are considering only the power generated by the fission in the fuel, which is the most important contributor.

As a first consideration, we see that power generation in the core due to fission is equal to 95.77 MW. Considering the almost 4 MW generated in the INVFS's, we end up with approximately 100 MW generated by fission.

The radial power distribution of the 68 FAs critical core is shown in Figure 3.12.

With respect to the INVFS' peaking factors [see Figure 3.8], the values referred to the core are clearly more homogeneous. Figure 3.13 allows us to compare our results with the ones referred to the 69 FAs 100 MW critical core.

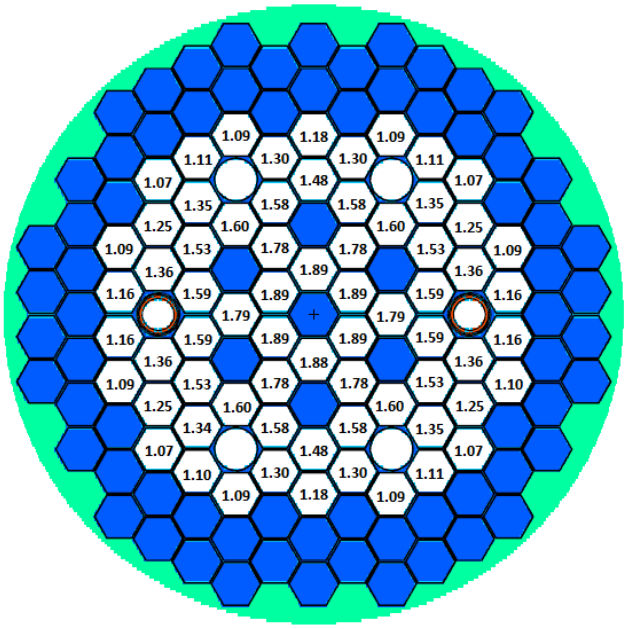

Figure 3.11: Power distribution in the core - Entire assembly, fissile part only. Values expressed in MW. Max standard deviation 0.05 %

Maximum power	1.89 MW
Average heat flux of the hottest FA	740.72 W/cm^2
Minimum power	1.09 MW
Average power	1.41 MW
Max radial peak factor	1.34
Highest axial peak factor	1.12
Axial peak factor in the hottest FA	1.12
Total power	95.66 MW

Table 3.5: Summary of the power parameters in the core

Figure 3.13 is obtained with the same assumptions made in our model, except for the fact that a cold density model was also adopted. Moreover, a different computer code has been used, namely ERANOS. Despite that, the found values are comparable, and this confirm the reliability of our results.

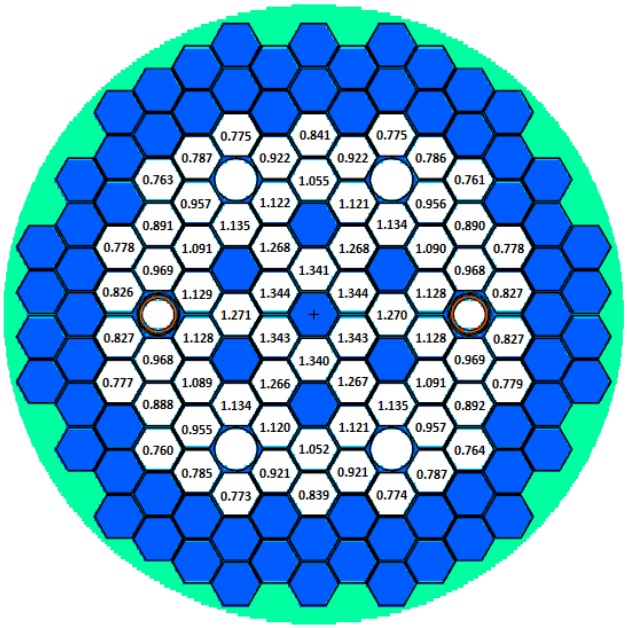

Figure 3.12: Power distribution in the core fissile zones. Relative error ± 0.001

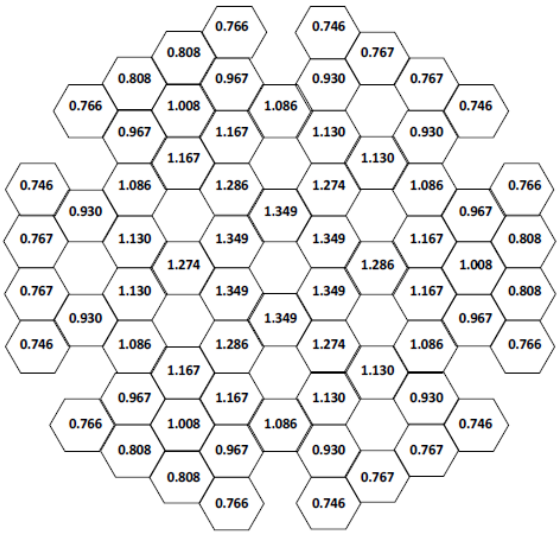

Figure 3.13: 100 MW-69 FA "BoL theoretical" core: power distribution ($ff_{rad-core}$) in the fissile zone with CR completely withdrawn (as at EOC, ERANOS/JEFF3.1). Courtesy of M. Sarotto [8]

3.6 Conclusion

In this chapter, both the flux and the power distribution in the INVFS's have been investigated. Thanks to the symmetry of the problem, the analysis was restricted to only one fuel storage.

The average neutron flux in the INVFS's is relatively high, of the order of $10^{13} neutrons/cm^2 s$. The radial peaking factor are however really high, showing that the flux in the INVFS's is strongly driven by the neutrons that leak from the core. On the other hand, the axial peaking factor are very low, showing an almost equal distribution of the flux along the active zone, and thus also of the power.

The analysis of the neutron flux averaged over the whole fuel assembly rather over the fissile part only has been accomplished as well, showing very similar results.

The thermal power analysis has obviously showed the same strong radial asymmetry already experienced for the flux distribution. The average power generated by one INVFS loaded with 76 fresh fuel assemblies, with the reactor in operation, is approximately equal to 1075 KW.

A flux and power map of the core was also carried on, in order to validate and compare the results of the INVFS's. From a comparison with the 69 FAs 100 MW critical core results, performed using the deterministic code ERANOS, the found values have shown to be reliable.

Chapter 4

Burn-up calculation

4.1 Introduction

The present chapter aims to provide an overview of the degradation of the fuel due to its storage in the INVFS's while the reactor is operating. Both fresh fuel and spent fuel, namely fuel that has already spent 5 cycles in the reactor, will be analyzed.

The fuel placed in the INVFS's have been divided in three groups, to take into account the different levels of irradiation, as shown in Figure 4.1.

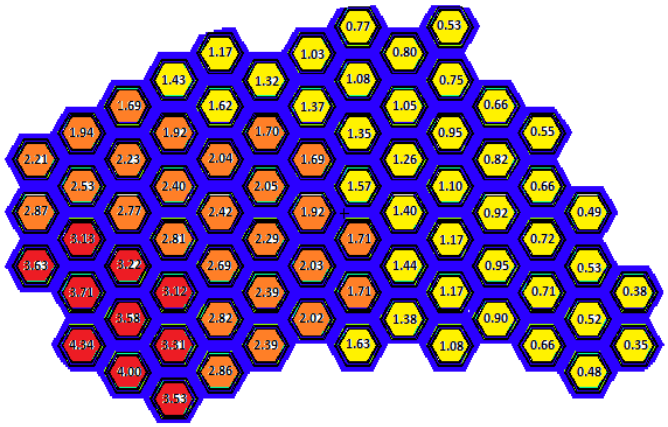

Figure 4.1: Division of the FAs in the INVFS as a function of the flux level

In order to divide the assemblies in the storage, the flux difference between the most and the less irradiated FA has been equally divided. We can notice again the strong dependence of the flux distribution in the INVFS's on the core leaking flux.

Table 4.1 illustrates the irradiation condition we are considering. As we can see, there is a mismatch between the average flux in one INVFS, calculated in the previous chapter by taking the average over all the assemblies, and the one computed by using the general purpose Monte Carlo burn-up code ALEPH [14]. Obviously infact, by grouping the FAs in only three zones we loose a bit of accuracy on the real irradiation conditions. Nevertheless, as we will see later, the differences are minimal.

	Number of FAs	Average neutron flux
Low irradiated	40	1.06E+13
Intermediate irradiated	26	2.42E+13
High irradiated	10	3.77E+13
Average flux in the INVFS 1.88E+13		
Average flux from previous chapter 1.74E+13		

Table 4.1: FAs repartition and irradiation condition

The cycle considered lasts 120 days, of which 90 are of irradiation and 30 of decay. Further informations on the model adopted can be found in Appendix B.

4.2 Fresh fuel

4.2.1 Initial composition of the fuel

Table 4.2 summarizes the initial composition of the considered fuel. A 33 % MOX fuel, which was foreseen for the 68 FAs critical core, was adopted. However, several changes in the fresh fuel composition have been made. The last 69 FAs critical core, for instance, is designed with a 34 % MOX fuel.

Isotope	Initial concentration (g/cm^3)	Percentage
O-16	1.245	11.79 %
U-235	0.045	0.43 %
U-238	6.197	58.70 %
Pu-238	0.072	0.68 %
Pu-239	1.746	16.54 %
Pu-240	0.829	7.85 %
Pu-241	0.187	1.77 %
Pu-242	0.236	2.24 %
Overall density: 10.557 g/cm^3		

Table 4.2: Initial composition of the fuel

We are thus dealing with a mixture of natural uranium oxide and 33 % Pu oxide. The most abundant Pu isotopes is the PU-239, with a percentage of 56.9 % over the total Pu present. The heavy metals represents the 88.2 % of the total, with a density of 9.312 g/cm^3.

4.2.2 Thermal power

The thermal power generation of the different FAs is listed in the table 4.3.

However, we are considering average irradiation condition. A more precise quantification of the power differences between the various FAs can be found in Chapter 3.4. Nevertheless, considering the uncertainties on the results already discussed in Section 3.2, the values found are fully consistent each other.

Period (days)	Low irradiated	Intermediate irradiated	High irradiated	Total (MW)
0	7.601	17.765	35.215	1.118
10	7.600	17.762	35.207	1.118
20	7.599	17.759	35.199	1.118
30	7.598	17.756	35.192	1.117
40	7.597	17.753	35.185	1.117
50	7.596	17.750	35.178	1.117
60	7.594	17.747	35.170	1.117
70	7.593	17.744	35.163	1.117
80	7.592	17.741	35.156	1.117
90	7.591	17.738	35.148	1.116
90-120	0	0	0	

Table 4.3: Thermal power (KW) for the different FAs as a function of time (days)

Nevertheless we have now the possibility to see the evolution of the thermal power in the INVFS's. As we expected from the flux map analysis, we almost have a constant evolution of the power. The more irradiated material, thanks to the higher fissile isotopes depletion, undergoes the higher decrease. However, it is easy to see that relative percentage difference is equal to:

$$\Delta\% = \frac{35.215 - 35.148}{35.215} = 0.190\%, \tag{4.1}$$

thus we can simply neglect it, and state that the thermal power in the INVFS's is constant.

After the operating period, the thermal power release drop immediately to zero, meaning that the decay heat in the INVFS's is negligible. Figure 4.2 shows graphically the behaviour of the power.

By multiplying the average thermal power release by the number of FAs, adding all the terms, we find that the overall thermal power of one INVFS is equal to 1.12 MW. This means that, according to this model, the thermal power generated in the four INVFS's is equal to the 4.468 % of the total reactor power. Considering the results found in the previous chapter, the total power generated in the four INVFS's is equal to 4.186 % of the total power. I encourage to use this last value to take into account the heat generation in the INVFS's, however the first one is for sure more conservative.

4.2.3 Burn-up

Table 4.4 shows the evolution of the burn-up for the various FAs.

Since we are dealing with fuel with a unique composition, thermal power release and burn-up are strictly related. The considerations previously expressed in chapter 4.2.2 are thus still valid.

4.2.4 Composition evolution of the fuel

It is of great importance the analysis of the composition evolution of the fuel, because it is necessary to verify whether the changes in the isotopes composition lead to the creation of

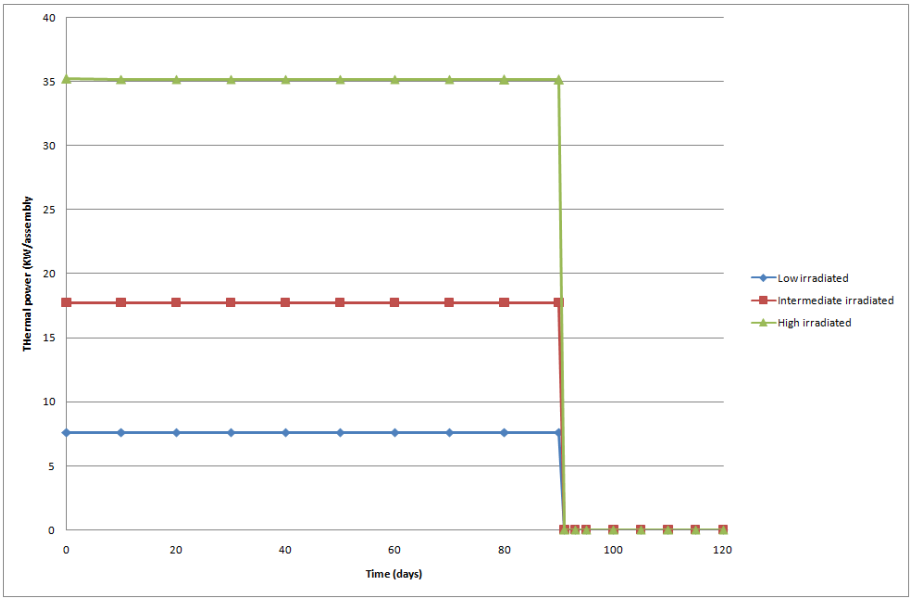

Figure 4.2: Thermal power evolution for the different FAs

Period (days)	Low irradiated	Intermediate irradiated	High irradiated
0	0	0	0
10	4.680	10.936	21.678
20	4.679	10.934	21.673
30	4.677	10.932	21.669
40	4.677	10.931	21.664
50	4.677	10.929	21.660
60	4.676	10.927	21.655
70	4.675	10.925	21.651
80	4.675	10.923	21.646
90	4.674	10.921	21.642
90-120	0	0	0

Table 4.4: Burn-up (KWd/Kg HM) for the different FAs as a function of time (days)

a fuel that eventually behaves differently in the core. Table 4.5 summarizes the evolution in the concentration of the initial nuclides of the most irradiated fuel. The O-16 evolution has not been reported, since its concentration remains constant.

Figure 4.4 provides a quicker understanding of the composition evolution.

As we can see, the fuel composition does not change markedly. Almost 90 % of the fuel depletion is due to the consumption of Pu-241.

The buildup of fission products and minor actinides is shown in figure 4.5.

While the build-up of the fission products stops after the end of the irradiation, the minor actinides keep on being produced, thanks to the not negligible activity of the Pu, and to the decay of the fission products themselves.

Finally, let's see the behaviour of fission products and minor actinides in the less irradiated FAs. As we can see in figure 4.6, the two curves are very similar, but of course the order

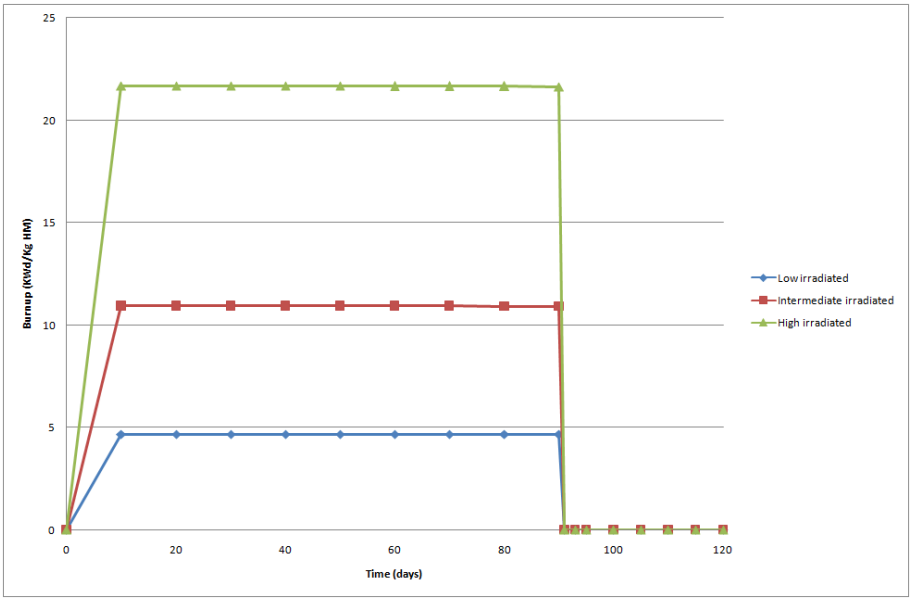

Figure 4.3: Burnup evolution for the different FAs

	U-235	U-238	Pu-239	Pu-240	Pu-241	Pu-242
0	0.04500	6.19700	1.74600	0.82900	0.18700	0.23600
10	0.04500	6.19683	1.74589	0.82901	0.18676	0.23599
20	0.04499	6.19665	1.74582	0.82901	0.18653	0.23598
30	0.04499	6.19648	1.74575	0.82902	0.18629	0.23598
40	0.04498	6.19630	1.74568	0.82903	0.18606	0.23597
50	0.04498	6.19613	1.74561	0.82903	0.18582	0.23596
60	0.04498	6.19595	1.74554	0.82904	0.18559	0.23595
70	0.04497	6.19578	1.74547	0.82905	0.18536	0.23594
80	0.04497	6.19561	1.74540	0.82905	0.18512	0.23594
90	0.04496	6.19543	1.74533	0.82906	0.18489	0.23593
91	0.04496	6.19541	1.74532	0.82906	0.18487	0.23593
93	0.04496	6.19541	1.74535	0.82906	0.18482	0.23593
95	0.04496	6.19541	1.74536	0.82906	0.18477	0.23593
100	0.04496	6.19541	1.74537	0.82906	0.18465	0.23593
105	0.04497	6.19541	1.74537	0.82906	0.18453	0.23593
110	0.04497	6.19541	1.74537	0.82906	0.18440	0.23593
115	0.04497	6.19541	1.74537	0.82906	0.18428	0.23593
120	0.04497	6.19541	1.74537	0.82905	0.18416	0.23593
Abs. diff.	-0.00003	-0.00159	-0.00063	0.00005	-0.00284	-0.00007
Rel. diff.	-0.07 %	-0.03 %	-0.04 %	0.01 %	-1.52 %	-0.03 %
Total transmutation of initial fissile material 1.69 %						

Table 4.5: Composition evolution of the fuel in g/cm^3 as a function of time (days)

of magnitude is lower.

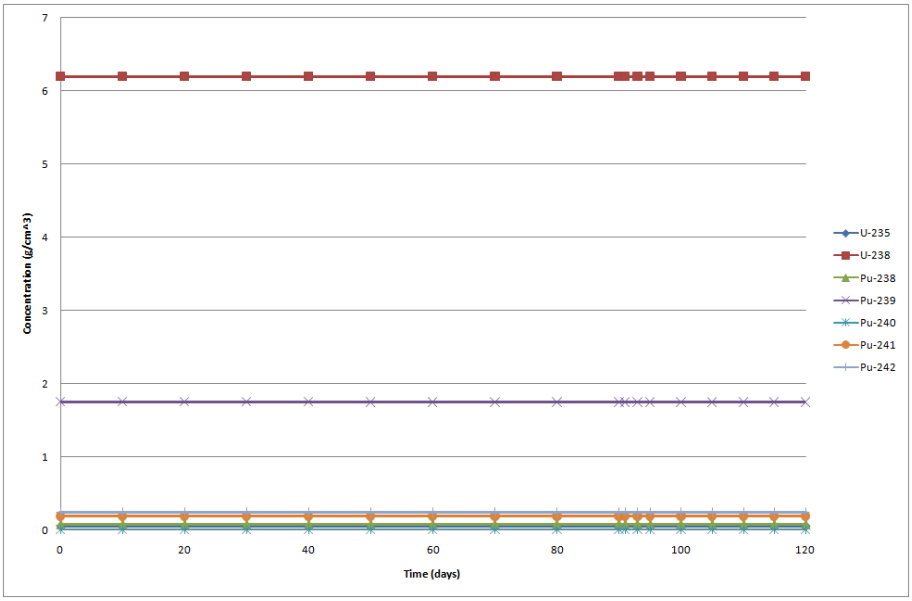

Figure 4.4: Composition evolution of the initial isotopes in the INVFS's most irradiated FAs

4.2.5 Evolution of the activity

In order to complete the analysis of the fuel, let's now see the evolution of its activity. We are particularly interested in this kind of information, to evaluate, for instance, whether a fresh fuel FA that has been one cycle in the INVFS's needs additional protection measures when it is handle due to its higher activity.

Figure 4.7 shows the evolution of the activity for the most irradiated FAs. As we expected, the major contribution comes from the fission products. Nevertheless, since we have build-up of only relatively short live fission products, their activity suddenly drop after the end of the irradiation. As a matter of fact, the total activity soon relaxes itself on the initial activity of the Pu.

The difference between the BoC and the EoC in terms of total activity is equal to 3.60 Ci/cm^3, with a relative difference of 17.0 %.

Regarding the less irradiated material, its evolution is shown in Figure 4.8

In this case, the activation of fission products is not even sufficient to overcome the natural activity of the Pu isotopes.

The difference between the BoC and the EoC in terms of total activity is equal to 0.63 Ci/cm^3, with a relative difference of 3.0 %.

We can thus conclude that the extra activity induced during one cycle is negligible, and does not represent a cause of additional protection measures.

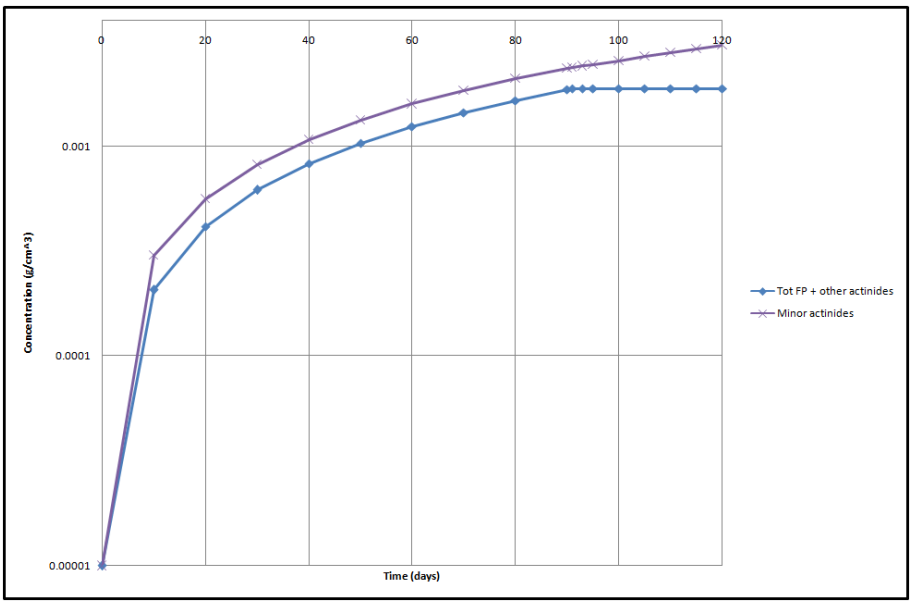

Figure 4.5: Composition evolution of FP and Minor Actinides in the INVFS's most irradiated FAs

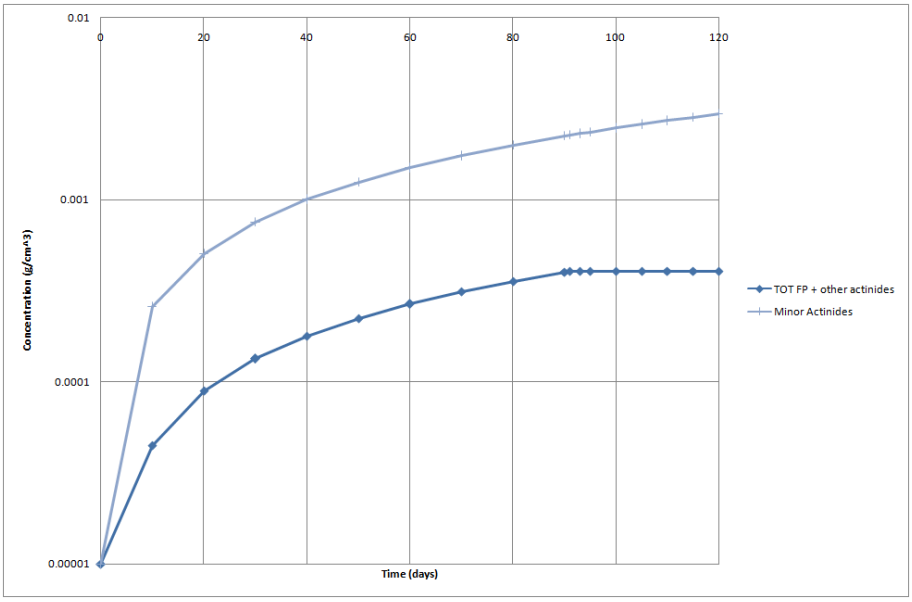

Figure 4.6: Composition evolution of FP and Minor Actinides in the INVFS's less irradiated FAs

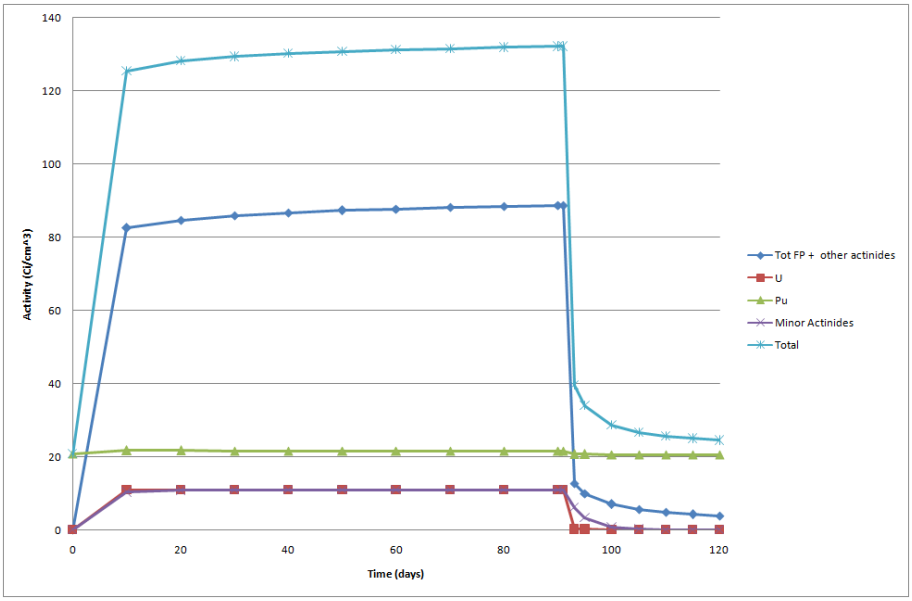

Figure 4.7: Activity evolution of the most significant groups of isotopes in the INVFS's most irradiated FAs

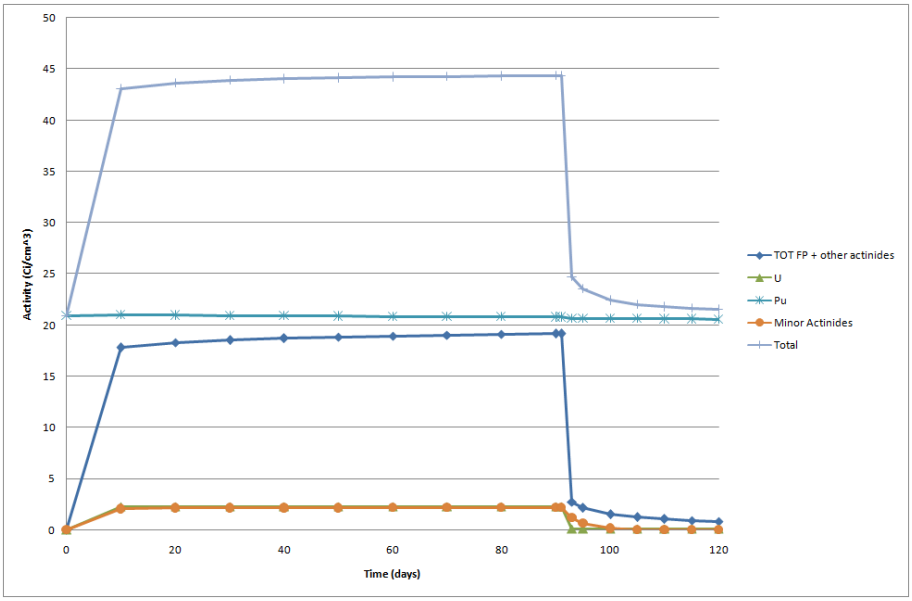

Figure 4.8: Activity evolution of the most significant groups of isotopes in the INVFS's less irradiated FAs

4.3 Irradiated fuel

To complete the discussion, let's now analyze the behaviour of spent fuel, namely fuel that has spent more than one cycle in the core, when it is stored in the INVFS's. The flux map in this case slightly change, so it has been considered in the following calculation a different repartition. See Table 4.6 for the value used.

	Number of FAs	Average neutron flux
Low irradiated	45	6.53+12
Intermediate irradiated	20	1.70E+13
High irradiated	11	2.89E+13
Average flux in the INVFS 1.31E+13		

Table 4.6: FAs repartition and irradiation condition

4.3.1 Initial composition

The fuel considered has spent 5 cycles in the reactor. From Table B.1, we know that after a cycle is composed of 90 days of irradiation, plus 30 days of decay, during which the reactor undergoes inspections and re-shuffle. After three cycles, however, a 90 days stop is foreseen in order to carry on major maintenance programme. Thus, the considered fuel has spent in total 450 days of irradiation and 210 of decay.

The initial composition of the fuel, listed in Table 4.7 has been provided from previously burn-up calculations.

It has to be noticed, in particular, the relatively high production of Am^{241} (0.45 % of the total, half-life of 432.2 years) and of Am^{243} (0.14 % of the total, half-life of 7370 years).

Table 4.7: Composition of the spent fuel

Isotope	Initial concentration (g/cm^3)	Percentage
80160	1.25E-01	11.88 %
330750	1.89E-07	0.00 %
340770	8.29E-07	0.00 %
340780	2.38E-06	0.00 %
340790	4.57E-06	0.00 %
340800	8.71E-06	0.00 %
340820	2.36E-05	0.00 %
350810	1.52E-05	0.00 %
360820	4.97E-07	0.00 %
360830	3.25E-05	0.00 %
360840	5.71E-05	0.01 %
360850	1.51E-05	0.00 %
360860	9.71E-05	0.01 %
370850	5.44E-05	0.01 %
370870	1.26E-04	0.01 %
380860	4.42E-07	0.00 %

Continued on next page

Table 4.7 – continued from previous page

Isotope[1]	Initial concentration (g/cm^3)	Percentage
380880	1.71E-04	0.02 %
380890	1.93E-05	0.00 %
380900	2.58E-04	0.02 %
390890	2.03E-04	0.02 %
390910	3.52E-05	0.00 %
400900	4.85E-06	0.00 %
400910	2.91E-04	0.03 %
400920	3.96E-04	0.04 %
400930	5.07E-04	0.05 %
400940	5.55E-04	0.05 %
400950	7.71E-05	0.01 %
400960	6.60E-04	0.06 %
410950	5.51E-05	0.01 %
420950	4.92E-04	0.05 %
420960	5.34E-06	0.00 %
420970	6.96E-04	0.07 %
420980	7.71E-04	0.07 %
420990	3.11E-09	0.00 %
421000	9.19E-04	0.09 %
430990	8.07E-04	0.08 %
441000	1.85E-05	0.00 %
441010	8.63E-04	0.08 %
441020	9.04E-04	0.09 %
441030	5.72E-05	0.01 %
441040	8.95E-04	0.08 %
441050	7.64E-16	0.00 %
441060	3.87E-04	0.04 %
451030	8.83E-04	0.08 %
451050	2.74E-12	0.00 %
461040	1.66E-05	0.00 %
461050	7.85E-04	0.07 %
461060	2.67E-04	0.03 %
461070	4.83E-04	0.05 %
461080	3.47E-04	0.03 %
461100	1.17E-04	0.01 %
471090	2.41E-04	0.02 %
471101	2.13E-07	0.00 %
471110	6.91E-08	0.00 %
481100	8.00E-06	0.00 %
481110	5.60E-05	0.01 %
481120	2.58E-05	0.00 %
481130	1.66E-05	0.00 %
481140	1.23E-05	0.00 %
481160	8.63E-06	0.00 %
491150	8.49E-06	0.00 %
501150	4.39E-07	0.00 %

Continued on next page

Table 4.7 – continued from previous page

Isotope[1]	Initial concentration (g/cm^3)	Percentage
501170	7.80E-06	0.00 %
501180	7.36E-06	0.00 %
501190	6.06E-06	0.00 %
501200	7.26E-06	0.00 %
501220	1.04E-05	0.00 %
501230	6.03E-07	0.00 %
501240	1.81E-05	0.00 %
501250	2.83E-08	0.00 %
501260	4.03E-05	0.00 %
511210	7.72E-06	0.00 %
511230	1.24E-05	0.00 %
511240	5.62E-08	0.00 %
511250	1.74E-05	0.00 %
511260	1.95E-08	0.00 %
521220	1.25E-07	0.00 %
521240	3.81E-07	0.00 %
521250	3.31E-06	0.00 %
521260	6.02E-06	0.00 %
521271	3.27E-06	0.00 %
521280	1.47E-04	0.01 %
521291	3.92E-06	0.00 %
521300	4.74E-04	0.04 %
531270	7.47E-05	0.01 %
531290	2.33E-04	0.02 %
531310	1.11E-06	0.00 %
541280	1.41E-06	0.00 %
541300	2.76E-06	0.00 %
541310	6.65E-04	0.06 %
541320	9.43E-04	0.09 %
541330	4.16E-07	0.00 %
541340	1.34E-03	0.13 %
541350	1.69E-15	0.00 %
541360	1.32E-03	0.13 %
551330	1.25E-03	0.12 %
551340	1.99E-05	0.00 %
551350	1.37E-03	0.13 %
551360	2.72E-07	0.00 %
551370	1.21E-03	0.11 %
561340	3.36E-06	0.00 %
561360	2.72E-05	0.00 %
561370	2.24E-05	0.00 %
561380	1.18E-03	0.11 %
561400	6.97E-06	0.00 %
571390	1.14E-03	0.11 %
571400	1.06E-06	0.00 %
581400	1.06E-03	0.10 %

Continued on next page

Table 4.7 – continued from previous page

Isotope[1]	Initial concentration (g/cm^3)	Percentage
581410	4.47E-05	0.00 %
581420	9.80E-04	0.09 %
581430	9.04E-13	0.00 %
581440	4.12E-04	0.04 %
591410	9.57E-04	0.09 %
591430	7.63E-06	0.00 %
601420	5.05E-06	0.00 %
601430	8.73E-04	0.08 %
601440	3.70E-04	0.04 %
601450	6.19E-04	0.06 %
601460	5.42E-04	0.05 %
601470	1.88E-06	0.00 %
601480	3.57E-04	0.03 %
601500	2.13E-04	0.02 %
611470	3.31E-04	0.03 %
611480	2.36E-08	0.00 %
611481	1.28E-06	0.00 %
611490	1.39E-10	0.00 %
611510	1.29E-14	0.00 %
621470	6.72E-05	0.01 %
621480	2.51E-05	0.00 %
621490	2.49E-04	0.02 %
621500	2.10E-05	0.00 %
621510	1.47E-04	0.01 %
621520	1.39E-04	0.01 %
621530	1.04E-11	0.00 %
621540	5.98E-05	0.01 %
631510	7.95E-07	0.00 %
631520	6.70E-08	0.00 %
631530	7.96E-05	0.01 %
631540	6.40E-06	0.00 %
631550	3.24E-05	0.00 %
631560	3.25E-07	0.00 %
641540	2.57E-07	0.00 %
641550	3.62E-06	0.00 %
641560	2.72E-05	0.00 %
641570	1.88E-05	0.00 %
641580	1.23E-05	0.00 %
641600	4.05E-06	0.00 %
651590	6.45E-06	0.00 %
661600	2.55E-07	0.00 %
661610	2.32E-06	0.00 %
661620	1.64E-06	0.00 %
661630	8.08E-07	0.00 %
661640	4.50E-07	0.00 %
671650	2.00E-07	0.00 %

Continued on next page

Table 4.7 – continued from previous page

Isotope[1]	Initial concentration (g/cm^3)	Percentage
681660	1.04E-07	0.00 %
681670	4.75E-08	0.00 %
922340	6.70E-05	0.01 %
922350	3.77E-03	0.36 %
922360	1.60E-04	0.02 %
922370	6.27E-08	0.00 %
922380	5.93E-01	56.22 %
932370	8.66E-05	0.01 %
932380	1.99E-11	0.00 %
932390	1.72E-08	0.00 %
942370	1.63E-08	0.00 %
942380	6.60E-03	0.63 %
942390	1.63E-01	15.44 %
942400	8.32E-02	7.88 %
942410	1.74E-02	1.65 %
942420	2.27E-02	2.15 %
942430	1.96E-20	0.00 %
952410	4.79E-03	0.45 %
952420	1.13E-09	0.00 %
952421	8.72E-05	0.01 %
952430	1.43E-03	0.14 %
962420	1.47E-04	0.01 %
962430	3.12E-06	0.00 %
962440	2.30E-04	0.02 %
962450	6.00E-06	0.00 %
982520	2.55E-21	0.00 %
Overall density 10.55 g/cm^3		

4.3.2 Thermal power

As shown in Figure 4.9 the thermal power generation is constant also when we consider spent fuel allocation. Comparing with the results referred to the fresh fuel, we can notice that we have lower power generation, meaning that the power due to fission also in the INVFS's overcomes the one due to radioactive decay. Considering the INVFS as a whole, the total power released with this kind of loading is equal to 723 KW. However, it is again important to remember that we are now considering three average irradiation conditions of the INVFS's, which lead to a not so accurate description of the various contributions.

[1]The isotopes are listed accordingly to the MCNPX symbolism: 10000*Z+10*A+M, with M=0 for ground and M¿0 for metastable states. For instance, 80160 represents Oxygen 16.

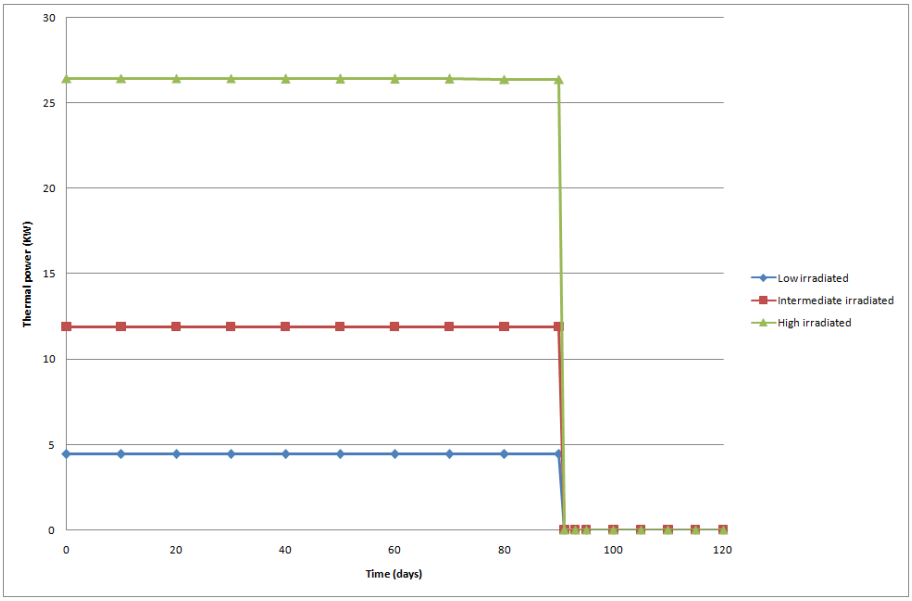

Figure 4.9: Thermal power evolution for the different FAs

4.3.3 Burn-up

The burn-up evolution is a strictly related with the power one. The results are shown in Figure 4.10

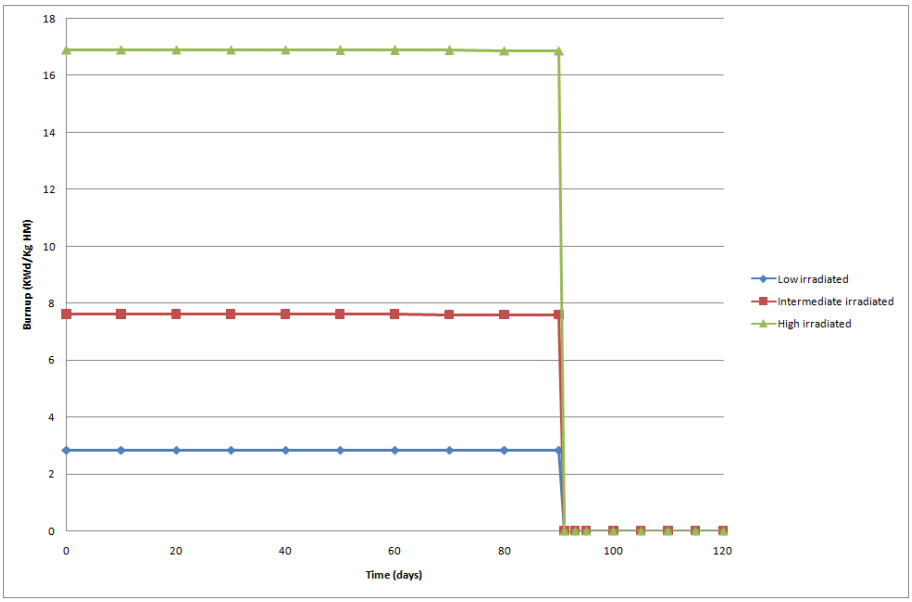

Figure 4.10: Burnup evolution of the spent fuel for the different FAs

4.3.4 Composition evolution of the spent fuel

Since we are now considering fuel that has spent several cycles in the core, under a flux that is two order of magnitude higher than the one we have in the INVFS's [see chapter

3.2], we do not expect significant changes in the fuel composition. Figure 4.11 summarized the results found.

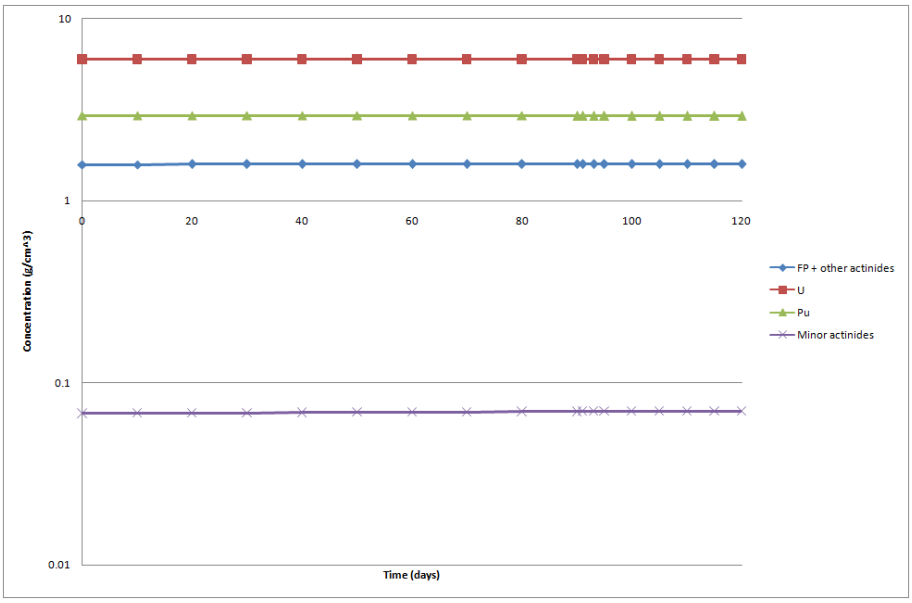

Figure 4.11: Composition evolution of the spent fuel in the INVFS's most irradiated FAs

Comparing with the fresh fuel results, we see that fission products concentration is now three order of magnitude higher, while the minor actinides concentration is roughly one order of magnitude higher.

Due to the basically constant evolution of the composition with time, the values referred to the less irradiated FAs were not reported.

4.3.5 Evolution of the spent fuel activity

This section will allow us to understand whether the activity of the spent fuel decreases, due to the radioactive decay, or increases, due to neutron activation, during the allocation in the INVFS's. The values that refers to the most irradiated fuel are shown in figure 4.12.

The total activity is mainly due to the decay of the fission products. At the beginning, we experience an increase of the activity, due to the decay of the most short-lived fission products. Afterwards we have a continuous decrease, which is nevertheless attenuated by the activation due to the flux. After 90 days, if we aim to handle this spent fuel, we have to tackle with a residual activity of approximately 100 Ci/cm^3, three times higher than the one present in the fresh fuel after 90 days of storage in the INVFS's.

4.4 Conclusion

The main goal of the present chapter was the investigation of the composition and activity of the fuel stored in the INVFS's. Both fresh fuel and spent fuel have been considered.

Concerning the fresh fuel, we have seen that its isotopes composition does not change remarkably. Fission products and minor actinides are produced approximately in the

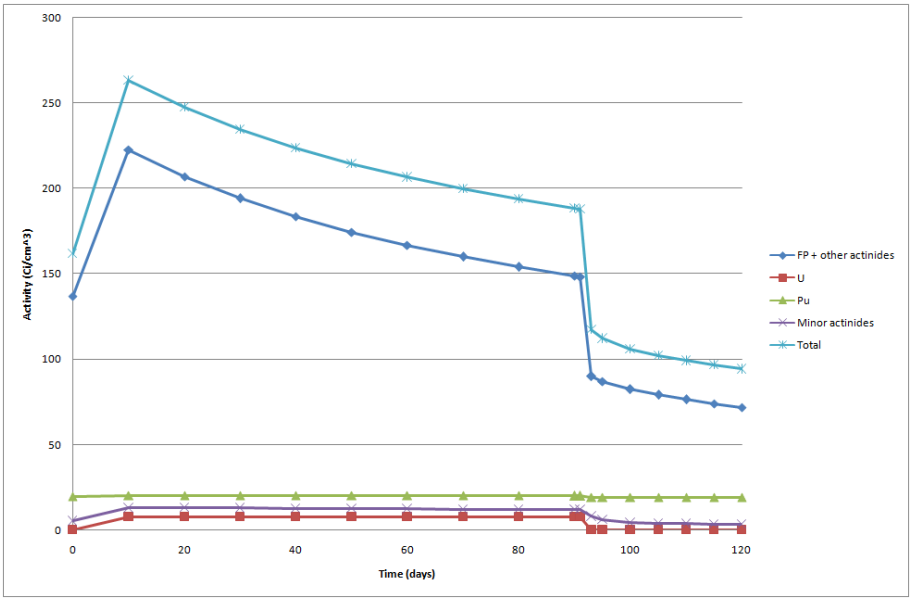

Figure 4.12: Activity evolution of the spent fuel in the INVFS's most irradiated FAs

same quantity, with the minor actinides a bit more abundant. The final concentration is however really small, of the order of 0.003 g/cm^3. No sensible change are observed between the less irradiated and the most irradiated fuel.

The activity is mainly driven by the activation of the fission products. The activation of U and minor actinides is relatively small, and also during irradiation remains below the natural activity of the Pu. After the 90 days of irradiation, the overall activity soon relaxes on the activity of the Pu, with only a slight increase. Thus, no further safety measurements have to be taken when handling this type of FAs.

Regarding the spent fuel, we have seen that the power generation is smaller than in the case of fresh fuel, as we expected. One In-Vessel Fuel Storage completely loaded with spent fuel generates approximately 720 KW, while in the case of fresh fuel loading the power is equal to approximately 1075 KW [see Chapter 3]. Thus it has been confirmed that, from a thermo-hydraulic point of view, the most crucial situation is reached when the INVFS's are loaded with fresh fuel assemblies.

The composition of the spent fuel loaded in the INVFS's for one cycle does not change sensibly. The activity, on the other hand, despite the irradiation, decreases, due to the decay of the high number of fission products produced while the fuel was in the core. From a starting activity of approximately 160 Ci/cm^3, the final value after 120 days is roughly speaking 100 Ci/cm^3.

A smart choiche, in order to decrease even more the depletion of the fresh fuel temporary loaded in the INVFS's, would be to allocate the spent fuel assemblies in the positions closer to the core and the fresh ones in the further, in order to create a shielding. In such a way, also the heat generation would be lower.

Chapter 5

Accidental condition analysis

5.1 Introduction

The demonstration of the safe behaviour of a nuclear power plant also during accidental conditions is a key point of the design. In this chapter, several severe accident conditions will be analyzed, mainly:

- the loss of cladding, while the fuel remains undamaged;
- the loss of cladding, with the fuel relocated as a "pancake" just beneath the top grid of the FAs;
- the loss of cladding, with the creation of a cladding cap at the top of the active zone and fuel relocated as a "pancake" beneath this cap;
- the partial loss of LBE around the central FAs of the core.

Besides that, different combinations of damaged FAs will be considered, both in the core and in the INVFS's.

Two important simplifications have been carried on during the following simulations, that is the same temperature and density for all the materials, independently by the operating conditions considered.

Moreover, a fourth accidental condition has been analyzed, namely the complete loss of the LBE in the reactor pool.

5.2 Loss of cladding

This situation represents the less severe type of accident, namely we consider that the over-temperature is sufficient to melt the cladding of the active part of the pin, but not high enough to melt the fuel, which remains in its original location. Moreover, we have assumed that the cladding is lost due to the drag of the LBE.

As a consequence, these assumptions lead to the filling of all the He filled gaps with LBE, which is thus in direct contact with the fuel. The reflector is assumed to remain in its original position.

Figure 5.1 helps to understand the new situation.

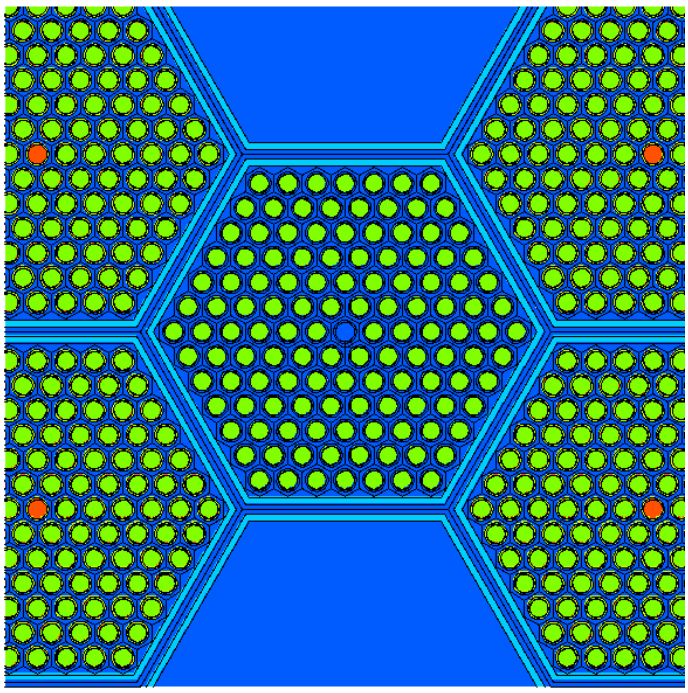

Figure 5.1: Damaged FA in the centre of the core, surrounded by undamaged FAs and IPS's

As we can see the central empty pin is now filled with LBE.

The same modifications have been carried on for the FAs in the INVFS's.

5.2.1 Results

Table 5.1 summarizes the three different scenarios that has been considered. First we have investigated the change in the reactivity following the damaged of a central FA in the core, and the hottest FA in each of the four INVFS's. Figure 5.2 shows the FA modified in the first INVFS.

Afterwards the results of the damage of all the FAs present in the core and finally the effects of the damage of all the FAs present in the four INVFS have been analyzed.

	k_{eff}	Standard deviation (pcm)
1 FA in the core, 1 FA in each INVFS	1.05346	11
All FAs in the core	1.08198	12
All FAs in the INVFS's	1.05241	11

Table 5.1: Criticality results in case of loss of cladding

Reminding that the k_{eff} of the core is equal to 1.05254 [Table 2.2], we conclude that we don't have sensible differences in the first and third scenario. On the contrary, the

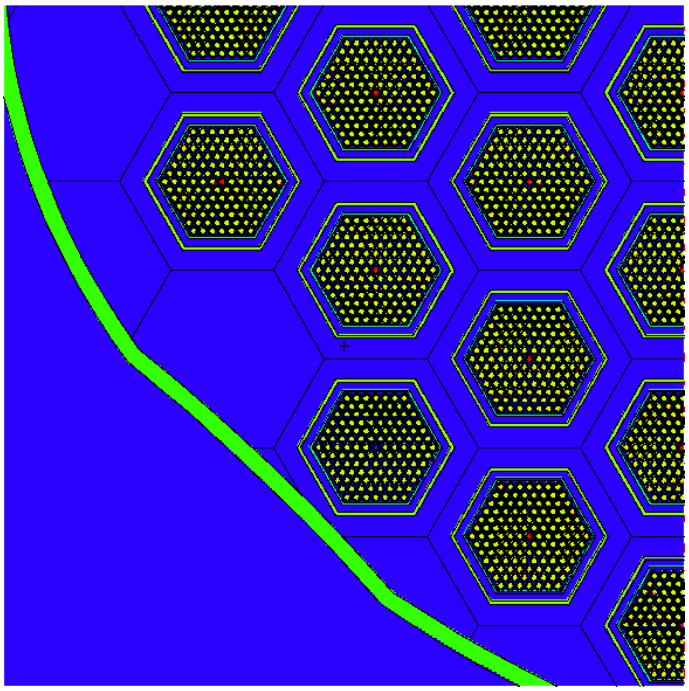

Figure 5.2: Cross section view of the FAs in the INVFS, with the FA without the cladding

complete damage of the core represents a more dangerous situation, because it would lead to an increase of the k_{eff} of 2944 pcm, with a reactivity of 7577 pcm [see Eq. 2.1]. However, since we are not considering now any kind of fuel relocation, we know that the control system is capable to insert approximately 11110 pcm of anti-reactivity in the core [see Chapter 2.4], thus this scenario doesn't represent a problem from a neutronic point of view.

5.3 Fuel relocation beneath the grid

A second accidental scenario that could occur is the melting of the fuel. In this case, the molten fuel, which has a density similar to the one of the LBE, could sink, float or be drag to the top. It has been chosen to consider this third situation.

The fuel has been thought to stop beneath the exit cone of the fuel assembly. In order to be consistent, the mass of molten fuel must be the same of the initial one. The volume of the fuel present in one fuel assembly is approximately equal to 1744 cm^3 [3.1]. Thus, since we assume equal density, this volume has to be relocated in the hexagonal cylinder below the cone, which has a pitch of 4.8775 cm. The height of the cylinder of fuel is then 21.165 cm. Figure 5.3 shows the relocation of the fuel, in the case of damage to the six central FAs of the core, while the rest remains intact.

In the following calculation, it has been also assumed that the CR assemblies, and the IPS's do not undergo any kind of melting, and they thus remain intact.

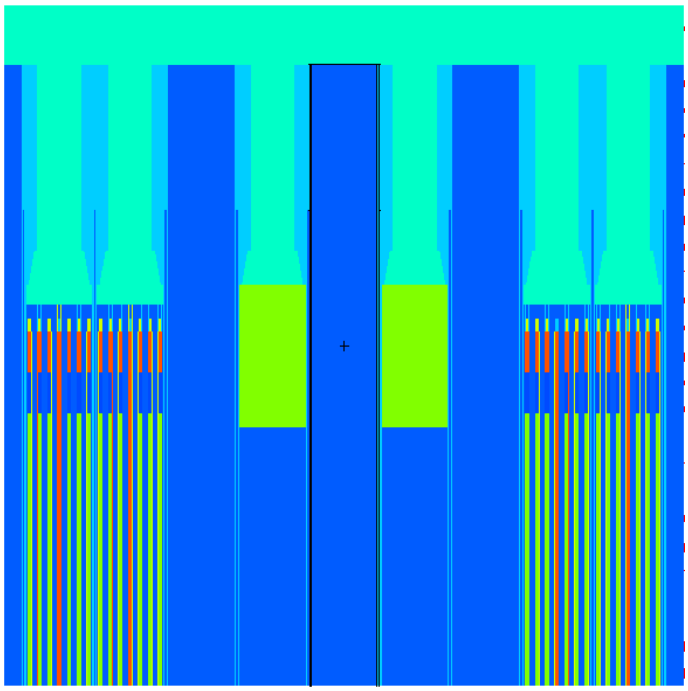

Figure 5.3: Relocation of the fuel beneath the grid: central FAs, rest of the core undamaged

5.3.1 Results

In this case, it was first analyzed the damage restricted to the 6 hottest FAs of the core. The INVFS are supposed to remain intact. Figure 5.4 shows a cross section of the core under these assumptions.

As a second step, the effect on the reactivity in case of total damage of the core and in case of total damage in the INVFS's has been calculated.

Table 5.2: Criticality results in case of loss of cladding and relocation of the molten fuel beneath the FA top grid

	k_{eff}	Standard deviation (pcm)
6 central FAs in the core	1.03708	12
All FAs in the core	1.27905	13
All FAs in the INVFS's	1.09707	15

As we expected, by comparing the obtained results with the previous ones, we immediately realized that we are now experienced a much more severe accident. While in the first case we have a decrease in the criticality, the second and the third case lead to very high level of the k_{eff}. This results does not have to surprise, since the melting of only a part of the core will lead in this case to the relocation of the fuel in an higher position, with loss of critical geometry.

It is thus necessary to verify whether the safety system is capable to maintain the reactor in a sub-critical condition in such a scenarios, taking also into account that the molten fuel is now in a higher position, and so the effectiveness of the control rods is reduced.

The table 5.3 shows the results obtained in a SCRAM configuration.

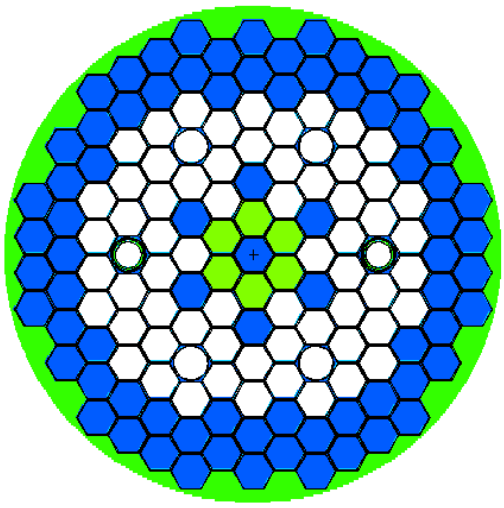

Figure 5.4: Cross section view of the core: central FAs damaged

	k_{eff}	Standard deviation (pcm)
All FAs in the core	1.20023	12
All FAs in the INVFS's	1.09750	12

Table 5.3: Criticality results in case of loss of cladding and relocation of the molten fuel beneath the FA top grid - SCRAM configuration

Thus, with the adopted model the system remains super-critical also with the insertion of all the six control-safety rods, which effectiveness is clearly limited by the new higher disposition of the fuel. By comparing the results of the total melting of the FAs in the INVFS's, we see that the k_{eff} basically does not change with the insertion of the CRs. This means that, in such a scenario, the criticality of the system is totally driven by the INVFS's, on which we do not have any kind of reactivity control.

Further study on this scenarios are thus strongly recommended. A more complete future accidental analysis should take into account thermo-hydraulic calculations, to verify if such an accident is realistic, together with more refined a neutronic analysis, which should consider also, i.e. the temperature and density change of the fuel and the materials that surround it.

5.4 Fuel relocation at the top of the active zone

A second severe accident evolution considered is supposed to lead to the creation of a "pancake" of fuel in the active zone.

In this scenario, the cladding of the active part is supposed to melt, but eventually solidify again at the top of the active part, creating thus a layer. The molten fuel is then supposed to be trap by the new barrier.

Figure 5.5 shows the two central molten FAs in the core. At the periphery is possible to notice part of two intact FAs.

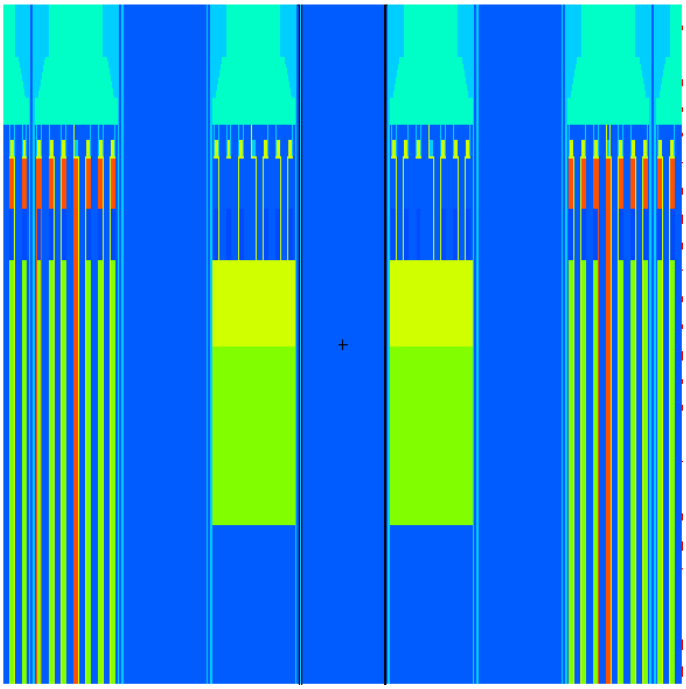

Figure 5.5: Front view of two molten FAs

	k_{eff}	Standard deviation (pcm)
6 central FAs in the core	1.09704	12
All FAs in the core	1.27281	13
All FAs in the INVFS's	1.10080	13

Table 5.4: Criticality results in case of loss of cladding and relocation of the molten fuel on the top of the active zone

To properly model this scenario, both the mass of the cladding and of the fuel has to be conserved. The relocation is thought to take place at the top of the active zone, so inside the 4.8775 cm pitch hexagonal cylinder. The volume of molten cladding is equal to approximately 840 cm^3, leading to a cylinder of 10.195 cm height. The height of the fuel cylinder is, as calculated previously, equal to 21.165 cm.

Again, both CR assemblies and IPS's are considered to remain undamaged.

5.4.1 Results

The same three scenarios already described in section 5.3 have been considered. Table 5.4 summarized the found results.

We have thus found again an extremely dangerous situation. The values of k_{eff} obtained are even higher than in the previous case, basically because now the molten fuel is compacted in the active part, so it is at the same height of the undamaged FAs. Here we have found an increase of the k_{eff} also when we have a partial damage of the core, because, on the contrary to the previous case, we are now considering a relocation of the fuel at basically the same height of the undamaged fuel pins.

Also in this case we are interested in verifying whether we are eventually able to reach a

sub-critical situation by inserting the control and safety rods. Table 5.5 summarizes the results in such a scenario.

	k_{eff}	Standard deviation (pcm)
6 central FAs in the core	0.97667	13
All FAs in the core	1.16424	13
All FAs in the INVFS's	1.10102	13

Table 5.5: Criticality results in case of loss of cladding and relocation of the molten fuel on the top of the active zone - SCRAM configuration

So only in the first case we are eventually able to go back to a sub-critical system, while in the other two cases the reactor remains strongly super-critical. Reminding the results found in Chapter 2.4, we know that in operational condition the SCRAM system is able to insert approximately 13000 pcm of anti-reactivity in the reactor. We thus see that the effectiveness of the CRs is slightly decreased, due to the compaction of the fuel. Also in this case, as we expected from the previous section analysis, there are not any kind of restoration effects if we suppose the total damage of the INVFS's.

5.5 Loss of coolant

An hypothetic total loss of coolant in the reactor represents one of the most severe accidents people could think on. The loss of the LBE will lead to the over-heating of the fuel, and eventually to its melting. The design of proper safety systems able to tackle this scenario is thus a crucial point.

Two different scenarios has been considered:

- partial loss of coolant in the hottest FA of the core;
- total loss of coolant in the reactor, SCRAM condition in the core.

5.5.1 Partial loss of coolant

An hypothetic accident scenario could involve the partial loss of coolant around the hottest FA in the core. Goal of this section is to investigate whether the effects of this event are considerable from a neutronic point of view.

Two different scenarios have been considered:

- loss of coolant around one central FA in the core;
- loss of coolant around the six hottest FA of the core.

In both the previous cases, different void fraction have been taken into account. The active zone have been divided in three zones along the height. For simplicity, let's call them zone A, B and C. Zone A contains the first 10 centimeters of the active part, starting from the bottom. Zone B contains the active part between 10 to 30 cm, while zone C contains the rest of the fuel pins, from 30 to 60 cm [see Figure 5.6].

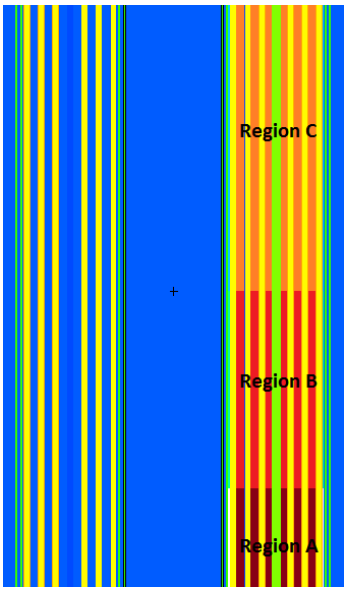

Figure 5.6: Frontal view of the active part of two fuel assemblies. On the right the three region considered are highlighted

Case 1	Zone A: 50 % LBE, Zone B and C: 100 % LBE
Case 2	Zone A and B: 50 % LBE, Zone C: 100 % LBE
Case 3	Zone A, B and C: 50 % LBE
Case 4	Zone A: 25 % LBE, Zone B and C: 50 % LBE
Case 5	Zone A and B: 25 % LBE, Zone C: 50 % LBE
Case 6	Zone A, B and C: 25 % LBE
Case 7	Zone A: 0 % LBE, Zone B and C: 25 % LBE
Case 8	Zone A and B: 0 % LBE, Zone C: 25 % LBE
Case 9	Zone A, B and C: 0 % LBE

Table 5.6: Summary of the different accident scenarios considered

Table 5.6 better explains the nine scenarios considered.

Figure 5.7 shows graphically the repartition of the different zones of depleted LBE along the channel height.

Table 5.7 refers to the case of loss of coolant in one central FA of the core.

Table 5.8 refers to the case of loss of coolant in the six central hottest FAs of the core.

We can easily notice that in both the two scenarios considered, the changes in the criticality are to all intents and purposes negligible. Since we do not experience sensible changes, the intermediate scenario in which we have a 25 % void fraction in the LBE has not been investigated.

Only in the hypothesis of total loss of coolant in the six central FAs of the core (Case 9, table 5.8), it seems that we start to have a clear increase in the reactivity (however, without a 99 % confidence level), but still the effect is minimal, and does not represent a cause of concern from a neutronic point of view.

Of course, a loss of coolant represents anyway a extremely severe accident, because may

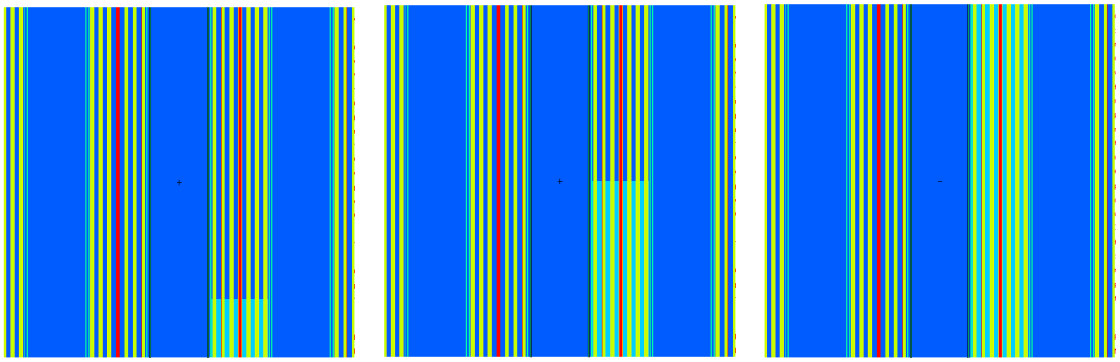

(a) 50 % LBE in the first 10 cm section, 100 % in the rest of the channel - Case1

(b) 50 % LBE in half of the channel, 100 % in the rest - Case2

(c) 50 % LBE in all the channel - Case3

Figure 5.7: Comparison between case 1, 2 and 3

	k_{eff}	Standard deviation (pcm)
Case 1	1.05269	12
Case 2	1.05270	12
Case 3	1.05276	11
Case 4	1.05266	12
Case 5	1.05265	11
Case 6	1.05264	11
Case 7	1.05277	11
Case 8	1.05262	12
Case 9	1.05276	11

Table 5.7: Loss of coolant in one central FA of the core

lead to the melting of the cladding and eventually of the fuel. However, we have here verify that the neutronic is unaffected by this scenario.

5.5.2 Total loss of coolant

From a neutronic point of view, we aim to verify whether this new configuration leads to an increase or a decrease of the k_{eff}, considering that all the LBE has been substituted by air.

The new operating conditions are not easy to define. A proper calculation should involved a parallel coupled work between the neutronic and the thermo-hydraulic part. In order to obtain a first order approximation result several assumptions have been made, summarized in table 5.9.

Apart from the air, which density has been change according to the perfect gas law, the densities of the materials have not been changed.

The value of k_{eff} found is equal to 0.74964, with a standard deviation of 10 pcm. Thus, in such a scenario we have a strong decrease in the reactivity of the reactor [see chapter 2.4 for reference values]. Nevertheless, even if we do not encounter reactivity problem, the

	k_{eff}	Standard deviation (pcm)
Case 1	1.05268	12
Case 2	1.05262	12
Case 3	1.05282	11
Case 4	1.05266	12
Case 5	1.05265	11
Case 6	1.05270	12
Case 7	1.05272	12
Case 8	1.05262	12
Case 9	1.05295	12

Table 5.8: Loss of coolant in the six central FAs of the core

Fuel temperature in the core	1800 K
Fuel temperature in the INVFS's	1200 K
Air temperature	1200 K
SS in the core	1500 K
SS in the INVFS's	550 K
Cladding in the core	1500 K
Cladding in the INVFS's	550 K

Table 5.9: Operating conditions in the case of loss of coolant

total loss of coolant remains the most severe accident people could think on, due to the melting of the structural materials and of the fuel.

Such an high decrease in the reactivity is due to the huge amount of leakeges in our system. In fact, thanks to the much lower total cross sections of the air with respect to the LBE, the escaped neutrons pass from a 1.2 % of the total lost neutrons[1] in our reference critical system, up to the 56.1 % in the case just analyzed.

5.6 Conclusion

In this chapter, several hypothetic accidental conditions have been analyzed, both affecting the FA in the core and in the INVFS's. A BoL configuration of the core, with fresh fuel assemblies in the INVFS's has been considered.

In the case of loss of cladding, the LBE is free to redistribute in strict contact with the fuel. Such a scenario leads to a sensible change of the reactivity only under the assumption that all the FAs in the core are damaged. However, the SCRAM is judged to be able to drive the system into a sub-critical state. In case that this accident occurs in all the FAs stored in the INVFS's, the effect is negligible.

A most severe class of accident involves the melting of the fuel. The fuel pins integrity is then lost, and the molten fuel is free to move. Two cases have been considered:

- relocation of the fuel beneath the top grid of the fuel assemblies;

[1] Namely, escaped, captured, loss to fission and (n,xn) reaction

- relocation of the fuel at the top of the active zone.

In both the two scenarios adopted, the fuel is thought to form a compact "pancake" inside the hexagonal pipe of the fuel assembly.

The present chapter did not aim to verify the feasibility of such scenarios, but is supposed to verify their effects.

Fuel relocation between the grid for the 6 central FA leads to a reactivity decrease due to increased local leakage and thus is from a neutronic point of view not a dangerous situation. Of course, when this happens in the total core or total IVFS, a more compact geometry is obtained that leads to a high reactive situation that cannot be counterbalanced by the shut-down system.

When the fuel relocation occurs at the centre of the core, a more reactive configuration is obtained. For the 6 central FA scenario, this can be countered by the shut-down system, but it cannot when it happens in the total core or IVFS.

According to the author, further study on these accidental situations should:

- verify whether we are dealing with realistic scenarios or if we are not;
- verify what are the damage's limits over which the actual safety system is not sufficient anymore to control the system;
- eventually provide modifications of the reactivity control system and/or core and INVFS's layout.

The last accident considered involved the presence of void coefficient in the LBE entering the central FAs of the core. Different level of voids have been considered, up to zero percent LBE. The analysis have not been carried on the whole core, but first on one fuel assembly, and then on the 6 central fuel assemblies of the core. The results do not show a clear significant trend, thus, form a neutronic point of view, this accident is not dangerous.

Finally, an extreme situation has been considered, namely the total loss of the LBE in the reactor pool. In this model the LBE has been replaced by air. The neutronic effect is in this case a strong reduction of the reactivity. The system becomes thus strongly sub-critical even without the insertion of the control rods.

Chapter 6

Conclusion

A pool reactor like MYRRHA foresees different devices in the pool itself, apart from the core. From a neutronic point of view, is then important to verify whether these installations affect the criticality of the reactor.

The present thesis has investigated the relations between the core of MYRRHA and the four In-Vessel Fuel Storages, under different configurations. The presence of devices such as pumps or heat exchangers has been judged to be negligible for a neutronic characterization purpose, and thus it was not considered.

The first important issue tackled was the verification of the presence of neutronic coupling between the core and the In-Vessel Fuel Storages. This phenomenon has been demonstrated to be negligible in all the configurations taken into account, namely normal operation and SCRAM conditions. Moreover, we have seen that the reactivity of the INVFS's themselves is well below the safety limit of $k_{eff} = 0.95$. Thus, with the actual design, the INVFS's do not represent a cause of concern from a neutronic point of view in Class I and II [15] operating conditions. The found results are in accordance with similar studies accomplished by the ITN group.

The second task handled was the flux and power characterization of the INVFS's. Accordingly with the previous results, a strong dependence upon the flux exiting from the core was found. The average flux in the INVFS's is on average two order of magnitude lower than the one present in the core. Nevertheless, the fuel assemblies closer to the core experienced a relatively high flux, up to $10^{14} neutrons/cm^2 s$. Under the assumption of loading an in-vessel fuel storage with 76 fresh fuel assemblies, the power generated in it, when the reactor is operating at the nominal power, is approximately equal to 1 MW. A short neutronic and thermal analysis of the reactor core has been carried on as well, mainly in order to validate the model adopted. It has been found a good agreement with previous calculations performed using the deterministic code ERANOS.

The fuel stored temporary in the INVFS's, despite it is not subjected to the harder conditions of the core, undergoes depletion due to the neutrons leaking from the core. However, in Chapter 4 it has been verified that this phenomenon is basically negligible, for both spent and, most important, fresh fuel. Also the activation of the fuel, mainly due to the build-up of fission products, is not significant, and soon relaxes on the normal activity of the fuel after the end of the 90 days irradiation period. The thermal analysis, carried on using this time the general purpose MONTE CARLO burn-up code ALEPH instead of MCNPX is in accordance with the results of Chapter 3. The heat generation in one

In-Vessel Fuel Storage completely loaded with spent fuel is approximately equal to 720 KW.

Finally, several accidental conditions were analyzed, affecting both the core and the IN-VFS's in various extent. Some considered scenarios lead to negligible or low changes in the overall reactivity, that is the loss of the cladding around the active part of the fuel pins or the appearance of void fractions in the LBE. The extreme situation in which all the LBE in the reactor pool is lost and substituted by air has been investigated as well. In such a case, the effect is a strong reduction of the reactivity, due to the very high neutron leakages from the system. More severe accidents, that could involve the melting of the fuel and its eventually re-compaction in a unique block, could lead to not controllable super-criticality. This, as it has been seen, appears to be a problem both in the core and in the INVFS's. Consequently, further studies on this scenarios are recommended, in order to verify to what extent the scenarios considered are realistic.

Appendix A

Reliability of the MCNP results

A.1 Introduction - Deterministic vs. probabilistic methods

The are mainly two way of solving complex differential equation, namely by using deterministic or probabilistic methods.

Deterministic methods, i.e. discrete ordinates, divide the space into small boxes, that eventually tends to infinitesimal volumes, and solve the differential equation for each of this small volume. We thus obtain information on the average behaviour of the quantity analyzed, i.e. particles transport.

Probabilistic methods on the contrary considered a subdivision of the system between events. The particles, in our case, are transported from an event to another, namely collisions, absorptions. To each of these events a certain probability is given, which depends on the type of interaction, material involved and energy of the two materials. The average behaviour of the particles is inferred by taking the average of the simulated particles, by means of the central limit theorem.

The central limit theorem states that given a certain number of independent and identically distributed random variables with expected value μ and variance σ^2, the sample mean $\bar{x} = \frac{1}{N}\sum_{i=1}^{N} x_i$ is normally distributed with mean μ and variance $\frac{1}{N}\sigma^2$, if N is sufficiently large. Thus, we know that for a number of simulations of the same experiment that tends to infinite, the error tends to zero, and our results match the exact mean of the phenomenon.

The advantages of probabilistic methods on the deterministic ones are then mainly two:

- they allow a detail representation of the physical spaces, since they do not require any kind of discretization of the space;
- in the hypothesis of having a infinitely powerful calculator, probabilistic methods are able to provide exact results.

A.2 Precision of the MCNP results

With the growth of the processor capabilities, the use of probabilistic methods has become more widespread. However, since it is impossible to run infinite number of simulations,

every probabilistic tally required the communication of the statistical error associated to it, in order to be meaningful.

MCNP provides a complete analysis of the statistical uncertainties associated with the results. Most of the methodologies used are not really user friendly, and will require quite a lot of time to analyze them all. Luckily enough, MCNP provides a final statistical check, where all these criteria are summarized, called the "Status of Statistical Check".

Although the user can simply check this summary, and see whether rely or not on the results obtained, I think is important to have a deeper insight of this aspect.

Aim of this section is to explain under which conditions we can rely on our results. It is assumed that the reader has a basic knowledge of statistic.

However, all the results presented in the thesis met all the statistical checks carried out by MCNP.

A.2.1 Confidence intervals

The confidence interval is the extimation of the range of values which is likely to include the unknown population parameter with a certain probability, called confidence level.

From the application of the Central Limit Theorem [22], we know that for a number of sampling that tends to infinite, if the random variables are generated with independent and identical initial distribution, the distribution of the sample mean values is a normal distribution. Then, the expected value lies in the confidence intervals:

$$\bar{x} - S_{\bar{x}} < E(x) < \bar{x} + S_{\bar{x}} \tag{A.1}$$

approximately the 68 % percent of the time, and in the confidence interval:

$$\bar{x} - 2S_{\bar{x}} < E(x) < \bar{x} + 2S_{\bar{x}} \tag{A.2}$$

approximately the 95 % of the time, with $S_{\bar{x}}$ extimated standard deviation.

However, it is crucial to point out that in case of bad sampling of the geometry or cross sections, it may be that both the sample mean and the extimated standard deviation are unknowingly wrong.

A.2.2 MCNP relative error

All the MCNP tallies are printed together with their extimated relative error, namely:

$$R = S_{\bar{x}}/\bar{x} \text{ [13]}, \tag{A.3}$$

where $S_{\bar{x}}$ is the estimated standard deviation of sample mean $\bar{x}$, defined as:

$$S_{\bar{x}}^2 = \frac{S^2}{N}, \tag{A.4}$$

where S is the standard deviation of the population x, and N is the number of sampling. Through this value, we have thus an immediate information on the width of the confidence interval, expressed as a fractional result with the respect to the extimated mean.

In order to rely in the obtained result, the value of R has to be lower than 0.05 [13].

A.2.3 MCNP Figure of Merit

The figure of merit (FOM) is a MCNP parameter defined as:

$$FOM \equiv \frac{1}{R^2 T}, \tag{A.5}$$

where T is the computer time used. By definition, R^2 is proportional to 1/N, while T should be proportional to N. Thus, for any Monte Carlo run, the FOM should be approximately constant.

The FOM is used a reliability indicator of the tally result. If the FOM is not approximately a constant (except for statistical fluctuations early in the problem), the confidence intervals may not overlap the expected score value [13].

The FOM can be used as an instrument in several other issues, like the optimization of the efficiency of a Monte Carlo simulation, or the extimation of the time required to reach a desired value of R. Nevertheless, this applications are behind the scope of this small appendix, and thus will be not explained.

A.2.4 MCNP Variance of the Variance

The variance of the variance is the extimated relative variance of the extimated R [13]. The advantage of such a parameter is the even higher sensitivity to fluctuations than R. By the definition previously expressed, we have that:

$$VOV = S^2(S_{\bar{x}}^2/S_{\bar{x}}^4. \tag{A.6}$$

In order to be confident in the reliability of our confidence interval, the MCNP manual suggests to obtain a VOV below 0.1.

A.2.5 The Empirical History Score PDF $f(x)$

In case of very large history scores, we can have statistical convergence on the basis of the previous parameters, but in reality we could have incorrect results due to bad sampling of the problem.

The empirical history Score probability density function $f(x)$ is an unknown PDF such that the quantity $f(x)dx$ is the probability of selecting a history score between x and $x+dx$ for the tally bin. The mathematical analysis of the problem is rather complicated, and it will be skipped. As a rule of thumbs, it has to be remembered that MCNP is confidence in the reliability of the result if the slope of $f(x)$ between the 25 and 201 history scores is greater than 3.

Appendix B

The Aleph model

B.1 Introduction

The burn-up analysis of the INVFS's was performed by using ALEPH, a Monte-Carlo burn-up code developed at the SCK-CEN, together with the JEFF-3.1.1 data library.

It uses steady-state Monte Carlo calculation of neutron fluxes and spectra, and then solves the system of Bateman equations for a given time step using the reaction rates calculated from these fluxes and spectra. Eventually, the nuclide concentrations are updated and passed to Monte Carlo driver for recalculation of fluxes and spectra [14].

In the following of this appendix the assumptions of the model will be explained.

B.2 ALEPH input options

During operation, MYRRHA is foreseen to work for 90 days, followed by a 30 days of inspection and re-shuffle [see Figure B.1].

Thus, it has been chosen to compute the burn-up of the fuel in the INVFS after 90 days of irradiation, followed by 30 days of decay. The time step between two constant power irradiation period has been set equal to 10 days. In our case, since the flux is constant, we did this choice to obtain at constant interval the values we looked for. During the dead period, we have shortened the time interval: 1 day, then twice 2 days, and eventually we took a measure every 5 days. This has allowed us to have a better understanding of the sharp evolution of the parameters after the end of the irradiation.

Three irradiation zones have been defined in the INVFS's, by taking the difference between the maximum and the minimum flux in them, and dividing this value by three.

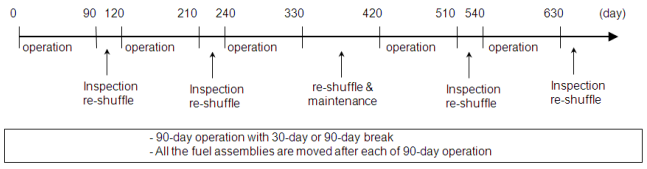

Figure B.1: Operation and maintenance scheme of MYRRHA [4]

The neutron flux is calculated by ALEPH by multiplying the tally track-length extimation of the flux of particles type l in a material k by the source strength.

$$\phi_{l,k} = S \cdot \varphi_{l,k}^{MCNP} \text{ [14]} \tag{B.1}$$

For an explanation of the source strength calculation, see Chapter 3.1.

The temperature of the fuel has been set equal to 900 K.

The energy range for the group structure goes from 1E-11 MeV to 20 MeV. 13400 fine energy groups have been used, with the following repartition:

Range of energy	Number of groups
1E-11 1E-10	1000
1E-10 1E-9	1000
1E-9 1E-8	1000
1E-8 1E-7	1000
1E-7 1E-6	1000
1E-6 1E-5	1000
1E-5 1E-4	1000
1E-3 1E-2	1000
1E-2 1E-1	2000
1E-1 1E+0	2000
1E+0 1E+1	200
1E+1 2E+1	200
Total number of groups 13400	

Table B.1: ALEPH energy groups

For the n^{th} group, the microscopic cross section is thus:

$$\sigma_g = \frac{\int_{E_{n-1}}^{E_n} \sigma(E)\varphi(E)dE}{\int_{E_{n-1}}^{E_n} \varphi(E)dE} \text{ [14]}, \tag{B.2}$$

with $\varphi(E)$ assumed to be constant between E_{n-1} and E_n.

Appendix C

Technical Note

C.1 Preamble

During this master thesis work, a simple calculation on the criticality of a MYRRHA FAs cluster has been requested from the safety analysis group.

The following work is not strictly related with the main topic of the thesis. Nevertheless, it has been decided to enclosed this technical note to the thesis, as a small "extra-work".

The provided template for the writing of the following document was written in Microsoft Word. This is the reason of the difference in the layout.

STUDIECENTRUM VOOR KERNENERGIE
CENTRE D'ETUDE DE L'ENERGIE NUCLEAIRE

ANS/NSP

G. Van den Eynde (2230

To:	cc:
☐ NN	☐ NN
☐ NN	☐ NN
☐ NN	

TITLE: Modelling of MYRRHA fuel assemblies behavior in case of water penetration into the storage
DATE: 6th July 2011

Abstract

The accidental condition when water penetrates into the MYRRHA fuel assembly storage was modeled.

The fuel assemblies were immersed into the big water tank in order to study the dependence of criticality from neutron moderation in water. Both fresh and spent fuel has been considered, with different loading configurations, up to the critical one.

.

Introduction

The safety of the fresh fuel assembly storage is a crucial point of the safety assessment. This short study aimed to investigate the fuel assembly behavior in case when water penetrates into the MYRRHA fuel assembly storage. The extreme conditions when the storage is fully filled with water were modeled by putting the cluster of fuel assemblies into the big water tank to model infinite neutron moderation in water and to study the criticality behavior under these conditions.

Calculation method

The calculation has been carried out by using the general purpose Monte Carlo radiation transport code MCNPX [1] with the pointwise neutron data library constructed from JEFF-3.1.1

library [2] for various temperatures. A cold geometry model of the fuel assemblies has been adopted. The temperature of all the materials has been set at 300 K, except for the fuel, that has been considered to be at 900 K.

The fuel assembly considered is the one forecast for the FASTEF 68 fuel assemblies critical core of MYRRHA (see reference [3] for a more detailed description). However, the central stiffness pin, He filled, has been replaced in these calculations with a normal fuel pin. The total number of fuel pins in one fuel assembly is thus equal to 127. The MOX fuel with 33 wt.% Pu in HM was used in this model. For the simplicity, the actual MCNPX model represents the MYRRHA core immersed into water instead of LBE.. A more detailed description of the geometry adopted can be found in Appendix A of [4].

The spent fuel resided 5 cycles in the core, for a total of 450 days of irradiation and 210 of decay. The fuel management is summarized in Fig.1.

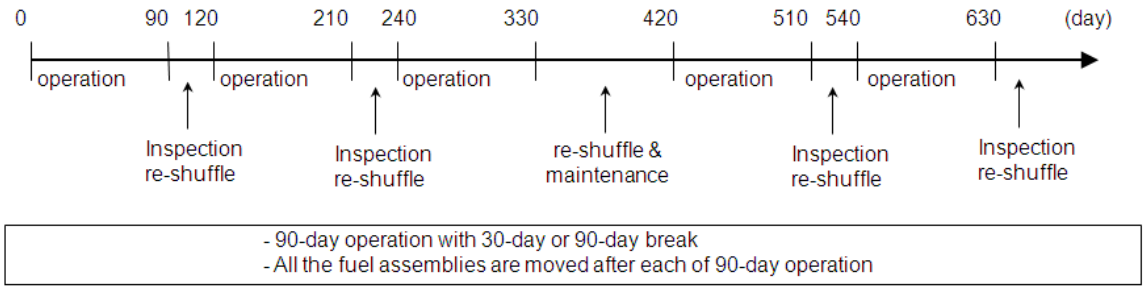

Figure 1 Fuel management of the MYRRHA core [5].

Results

The results for the fresh fuel storage are shown in Figure 2.

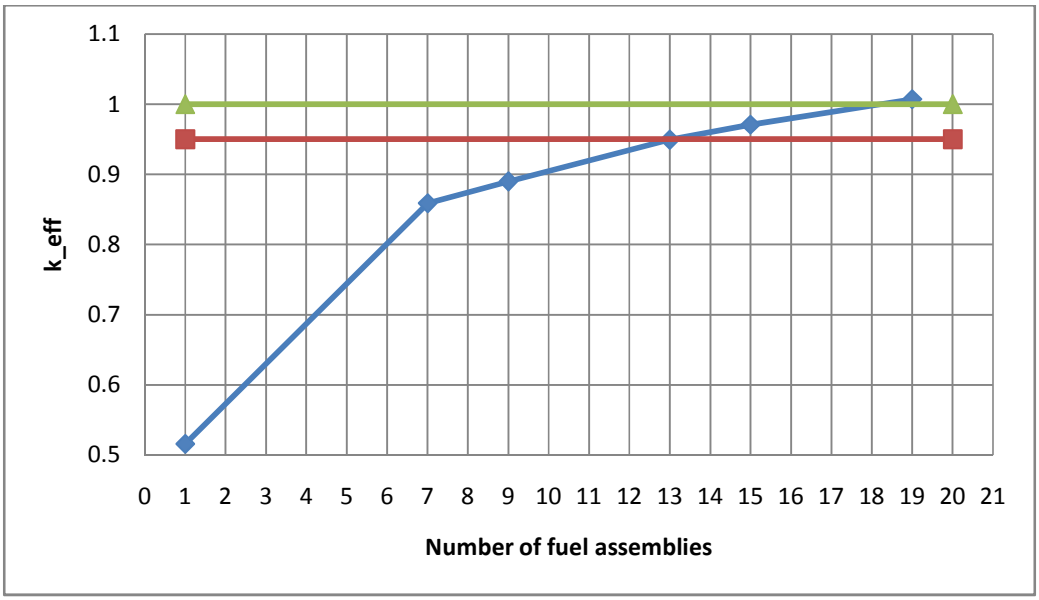

Figure 2 Fresh fuel criticality evolution as a function of the number of fuel assemblies

As it is seen,, the system is critical with 19 fuel assemblies. A cross section view of this 19 fuel assemblies system is depicted in Figure 3.

# FA	k_eff	Stand dev
1	0.51621	0.00117
7	0.85856	0.00133
9	0.88971	0.00128
13	0.94913	0.00132
15	0.97073	0.00128
19	1.00699	0.00128

Table 1 Summary of the fresh fuel results

The k_eff limit of 0.95 is not exceeded with 13 FAs, On the other hand we can state with 99 % confidence level that with 19 FAs configured as shown in Figure 3 the system is critical.

The configuration with13 fuel assemblies is shown in Figure 4.

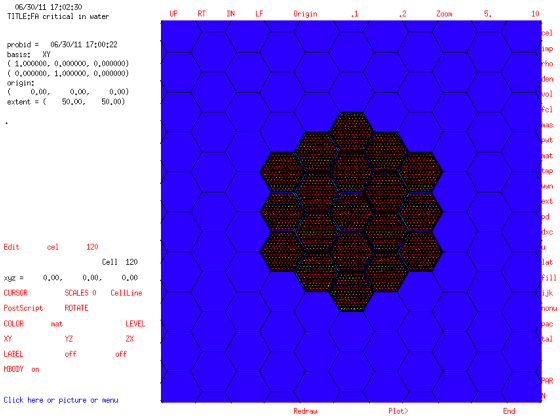

Figure 3 Critical 19 FAs configuration

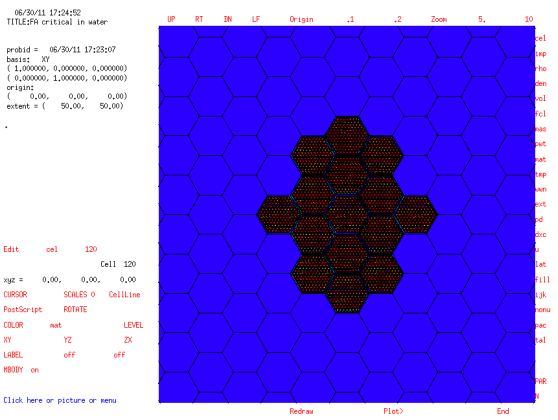

Figure 4 13 FAs configuration

Regarding the spent fuel, there is a possibility to store more fuel assemblies before reaching the criticality. With 19 FAs in the configuration of Figure 3, the system has a k_eff equal to 0.90348 with a standard deviation of 118 pcm.

The results of the calculation with the spent fuel are shown in Figure 5.

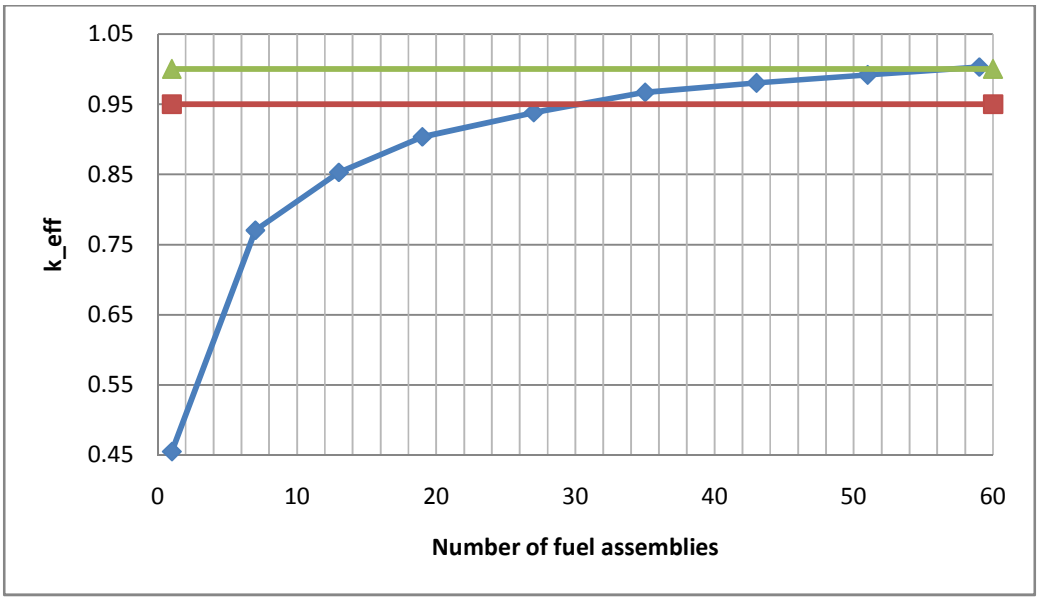

Figure 5 Spent fuel criticality evolution as a function of the number of assemblies

The criticality is reached with 59 fuel assemblies. The k_eff = 0.95 safety limit is crossed with approximately 30 FAs. Thus, roughly speaking , the limit is three times higher with respect to the fresh fuel results.

# FA	k	stand dev
1	0.45501	0.00102
7	0.77015	0.00117
13	0.85268	0.0013
19	0.90348	0.00118
27	0.93801	0.00111
35	0.9668	0.00116
43	0.98029	0.00119
51	0.99183	0.00118
59	1.00272	0.00121

Table 2 Summary of the spent fuel results

Figures 6 and 7 show the 27 and the 59 FA critical configurations adopted in the model.

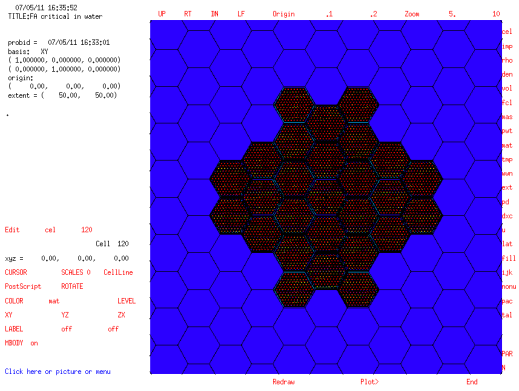

Figure 6 27 FA configurations

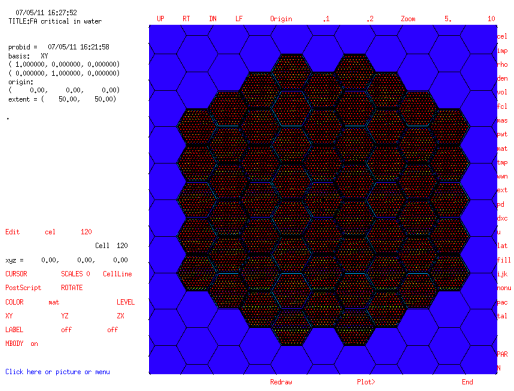

Figure 7 Critical 59 FA configurations

Conclusion

In this report the criticality behavior of the MYRRHA fuel assemblies at the condition when water penetrates into the storage has been investigated. The group of 19 fresh fuel assemblies is critical in case of infinite water moderator. Storage of spent fuel under these conditions is much less problematic. Nevertheless, also in this case the system reaches the criticality if 59 fuel assemblies are stuck together.

References

1. Pelowitz, D. B., ed., "*MCNPX User's Manual, Version 2.6.0*," LA-CP-07-1473 (2008).
2. Santamarina, A., *et al.,* ed., "*The JEFF-3.1.1 Nuclear Data Library, JEFF Report 22*," NEA No. 6807, OECD (2009).
3. Sarotto, Massimo, "*Design changes for FASTEF to operate in a critical mode*", Brussels (SCK-CEN), 14-15th October 2010.
4. Benedetti, Stefano, *"Neutronic coupling between the core of MYRRHA and the in-vessel fuel storage – Confidential version"*, BNEN Master Thesis, August 2011.
5. Abderrahim, H. Aït, *"Accelerator Driven System-BNEN Seminar"*, Mol, November 2010.

Bibliography

[1] L. Verwimp and A. Verledens. *SCK-CEN 1952-2002*. Promotional brochure, 2002.

[2] H. A. Abderrahim, A. Al Mazouzi, B. Arien, P Baeten, D. De Bruyn, D. Maes, E. Malambu, P. Schuurmans, M. Schyns, V. Sobolev, G. Van den Ende, D. Vandeplassche. *Myrrha technical description*. SCK-CEN, Boeretang 200, B-2400 Mol, Belgium, October 2008.

[3] Fernandez R. *MYRRHA Primary System*. SCK-CEN Presentation, 2010.

[4] Fernandez Rafael, *et al., MYRRHA Primary System Technical Description - Preliminary Draft*. SCK-CEN, June 2011.

[5] Lamarsh, John R. *Introduction to nuclear reactor theory*. Addison-Wesley, 1972.

[6] Pelowitz, Denise B. *MCNPX User's Manual, Version 2.6.0*. November 2007.

[7] mcnpx.lanl.gov

[8] Sarotto, Massimo et al. *Critical core design of MYRRHA-FASTEF: refinement of shutdown systems and neutronic characterisation of the equilibrium sub-cycle core*. ENEA Technical Report UTFISSM-P9P0-011, June 2011.

[9] AA.VV. *Handbook on Lead-bismuth Eutectic Alloy and Lead Properties, Materials Compatibility, Thermal-hydraulics and Technologies*.

[10] Beeley, Philip. *Nuclear criticality safety management*. Nuclear department DCEME HMS Sultan, 2005. OECD/NEA Report No. 6195, 2007.

[11] Sarotto, Massimo. *Design changes for FASTEF to operate in a critical mode*. Brussels (SCK-CEN), 14-15th October 2010.

[12] Di Maria, S. & Vaz, P. & Teles, P. & Romanets, Y. *In Vessel Fuel Storage criticality assessment: preliminary results (task 2.1)*. Brussel, 14-15th October 2010.

[13] X-5 Monte Carlo Team. *MCNP-A general Monte Carlo N-Particle Transport Code, Version 5*. Los Alamos national laboratory, 2003.

[14] Stankovskiy, A. & Van den Eynde, G. *ALEPH 2.1 A Monte Carlo Burnup Code*. SCK-CEN open report, February 2011 .

[15] Van Hove, Walter. *Operation and Control* BNEN Course. Mol, April 2011.

[16] Santamarina, A., *et al.,* ed,. *The JEFF-3.1.1 Nuclear Data Library, JEFF Report 22*. NEA No. 6807, OECD (2009).

[17] Ottolini, Marco. *CDT:WP2 T2.1 in Mol. Design of FASTEF in Sub-critical & Critical Mode*. CDT-WP2 meeting. SCK-CEN Brussels, January 19-21th, 2011.

[18] Abderrahim, H. A. *Accelerator Driven System-BNEN Seminar*. Mol, November 2010.

[19] Duderstadt, James J. & Hamilton, Louis J. *Nuclear reactor theory*. John Wiley and Sons, 1976.

[20] Abderrahim, H. A. *Nuclear Reactor Theory Part III - BNEN course*. Mol, Academic Year 2010-2011.

[21] Dubi, Arie. *Basic concepts of the Monte Carlo method*. Ispra seminar, 1984.

[22] Spanier, Jerome & Gelbar, Ely M. *Monte Carlo Principles and Neutron Transport Problems*. Addison-Wesley, 1969.

[23] Shane P. Pederson. *Mean Estimation in Highly Skewed Samples*. Los Alamos National Laboratory Report LA-12114-MS (1991).

[24] Stabin G. Michael. *Radiation protection and dosimetry* Springer, 2008.

[25] Peetermans, Steven. *Windowless spallation target - proton beam interaction study in the Myrrha reactor*. BNEN Master Thesis, August 2010.

[26] Vázquez M., Martín-Fuertes F., Álvarez Velarde F. *Core and IPS analysis with the official MCNP reference model*. WP2 FP7 CDT Meeting, SCK-CEN, Mol, May 2011.

[27] Malambu, Edouard. *FASTEF Core Physics Design - Critical Core*. WP2 FP7 CDT Meeting, SCK-CEN, Mol, May 2011.

[28] Dagan, R., Becker M., Schikorr M., Travleev A. *Subcritcal reactor scoping analysis*. WP2 FP7 CDT Meeting, SCK-CEN, Mol, May 2011.

[29] Sarotto, Massimo. *Design changes for FASTEF to operate in a critical mode*. WP2 FP7 CDT Meeting, SCK-CEN, Mol, May 2011.

[30] Sarotto, Massimo et al. *Critical core design of MYRRHA-FASTEF: main reactivity coefficients at BoL, BoC and EoC - Draft Version*. ENEA Technical Report UTFISSM-P9P0-012, June 2011.

[31] Travleev, A. *Feedback coefficients for subcritical FASTEF core*. WP2 FP7 CDT Meeting, SCK-CEN, Mol, May 2011.

[32] Di Maria S. et al. *Neutronic characterization and decay heat calculations in the In-Vessel Fuel Storage Facilities for the CDT Project*. Instituto Tecnologico e Nuclear, EN 10, 2686-953 Sacavém, Portugal.

[33] Van den Branden G., Van den Eynde G. *Master Thesis Project Guidelines*. SCK-CEN, Academic year 2007-2008.